CENTRO DE INVESTIGACIÓN Y DE ESTUDIOS AVANZADOS DEL INSTITUTO POLITÉCNICO NACIONAL

Unidad Monterrey

Development of a microfluidic device for cell capture, stimulation, and protein secretion detection.

Tesis que presenta

Roberto Rodríguez Moncayo

para obtener el grado de Maestro en Ciencias en

Ingeniería y Física Biomédicas

Director de tesis

Dr. José Luis García Cordero

Apodaca, Nuevo León Agosto de 2016

Acknowledgements

I would like to thank my thesis supervisor, Dr. José Luis García Cordero, for all the opportunities provided, but most importantly, for all his support and guidance through this exciting world of microfluidics. I would also like to thank the Consejo Nacional de Ciencia y Tecnología (CONACyT), for the scholarship and grants that made this project possible. A thank you goes to CINVESTAV-Monterrey, for the facilities, the help, and the knowledge provided to me.

I would like to thank my family and Diana Cedillo for all the love and support, I would have not done it without you. Lastly, I would like to extend my appreciation to my laboratory mates, for all the cakes we shared together.

Table of contents

Abstract

Cellular behavior is governed by the secretion of different molecules in response to environmental cues. These molecules transmit information between cells, and orchestrate a host of responses, including proliferation, migration, and cell death. Of special interest is the secretion of cytokines, small proteins that coordinate the immune response, that mediate intercellular communication. These proteins can also be used as biomarkers for conditions ranging from cancer to autoimmune disorders.

The placement of a protein biosensor next to stimulated secretory cells could provide information regarding pathological states, efficacy of prescribed drugs, and general cellular physiology and metabolism. Microfluidics opens up the possibility of reaching this level of integration. Although cell patterning methods and protein biosensors have been developed at the microfluidic scale, there are currently not many examples of microfluidic devices integrating both methods in a single device.

In this work, we present a PDMS microfluidic device for cell capturing and protein detection. The microfluidic device integrates a biosensor next to a cell patterning method, and an on-chip stimuli delivery system, both enabled with pneumatic microstructures. We were able to trap and isolate monocytes in 64 assay chambers, with the number of captured cells increasing as a function of both seeding time and cell concentration. Furthermore, we were able to perform a proof-of-concept immunoassay utilizing a fluorescent protein, suggesting that, in principle, the microfluidic device could be used to measure cytokine secretion from a previously captured cell population.

Resumen

El comportamiento celular está gobernado por la secreción de diferentes moléculas en respuesta a señales ambientales. Estas moléculas transmiten información entre células y orquestan una variedad de respuestas, incluyendo proliferación, migración y muerte celular. De interés espacial es la secreción de citocinas, proteínas pequeñas que coordinan la respuesta inmune, que median la comunicación intercelular. Estas proteínas también pueden ser utilizadas como biomarcadores para condiciones que van desde el cáncer hasta desordenes autoinmunes.

La colocación de un biosensor de proteínas junto a células secretoras puede proveer información correspondiente a estados patológicos, eficacia de fármacos prescritos, y fisiología y metabolismo celular general. La microfluídica abre la posibilidad de alcanzar tal nivel de integración. Aunque métodos de captura celular y biosensores de proteínas han sido desarrollados en la escala microfluídica, en la actualidad no hay muchos ejemplos de dispositivos microfluídicos integrando ambos métodos en un solo dispositivos.

En este trabajo, presentamos un dispositivo microfluídico de PDMS para captura celular y detection de proteínas. El dispositivo microfluídico integra un biosensor junto a un método de captura celular, así como un sistema de entrega de estímulos en chip, ambos activados con microestructuras neumáticas. Fuimos capaces de atrapar monocitos en 64 cámaras de ensayo, con el número de células capturadas incrementando en función tanto del tiempo de siembra como de la concentración celular. Además, fuimos capaces de desarrollar un inmunoensayo como prueba de concepto utilizando una proteína fluorescente, sugiriendo que, en principio, el dispositivo microfluídico puede ser utilizado para medir secreción de citocinas de una población celular previamente capturada.

1 Introduction

The way information is relayed to and from a cell is called cell communication. This information exchange can occur between a cell and its environment or itself. The cellular microenvironment is dynamic, so the cell must adapt to these conditions by adjusting its internal biochemical processes in order to survive. Metabolic pathways are switched on or off depending on the available source of nutrients. Signaling pathways are activated in response to external signals, which can also alter the way genes are expressed. Not only does the environment act upon a cell, but the cells have also the ability to modify its environment, for example, by increasing the production of specific biomolecules [1].

1.1 Types of intercellular communication

Intercellular communication can be carried out through direct contact or by soluble factors. An example of a direct contact communication is gap junctions, these junctions allow the exchange of intrinsic biomolecules between a cell and an adjacent cell through specialized channels. Another example is the interaction of proteins on the plasma membrane of adjacent cells, which activate signaling cascades in either one of the cells [1].

On the other hand, cell-cell communication through soluble factors can either act locally or at a distance. Local communication encompasses autocrine and paracrine signaling, in which a cell can act upon itself or cells in the vicinity, respectively. Communication at a distance is also called endocrine signaling [1]. Examples of endocrine signaling includes the secretion of hormones into the circulatory system, which carries them to target cells throughout the whole body [1], and monocytes (a type of white blood cells) releasing Interleukin-1 which bind to receptors on their membrane [2]. Local concentrations of growth factors that dictate

proliferation and differentiation, and are especially important during embryonic development, is a type of paracrine communication [3].

Cell communication have been studied using reductionist or holistic approaches. In a reductionist approach, cells from a tissue are cultivated *in vitro*, subjected to a specific signal and their response measured. In contrast, a holistic approach involves the study of an organism *in vivo*, subjecting it to a specific agent that will either activate or inhibit a response, and samples from the area of interest in the organism are taken and analyzed. Traditionally, cellular biology studies utilize a reductionist approach [4].

1.2 Immune system and cytokines

The immune system is an assembly of cells, tissues and organs that protect the body against invading pathogens and disease. The immune system must be highly regulated: imbalances in its regulatory mechanisms can result in autoimmune disorders, inflammatory diseases or cancer [5]. This regulation is mainly achieved is by communication through soluble factors [6].

Cytokines are small proteins released mostly by immune cells [7], and are responsible for information exchange between the immune cells and the environment [8]. There are several families of cytokines, each specialized in eliciting different responses over the receiving cells. The interleukin (IL) family regulates mainly cell growth and differentiation of immune cells [9]. The tumor necrosis factor (TNF) family is a set of anti-tumorigenic proteins that induce cell death [10]. Chemokines regulate cell migration and activation [11]. Interferons (IFN) released by virus-infected cells and cancer cells, increase host defenses [12].

The coordinated release of different cytokines can induce a pro-inflammatory or an anti-inflammatory response. An example of a pro-inflammatory process is

when bacteria enters a tissue, cells in the surrounding area will start releasing chemo-attractant molecules (*e.g.* IL-8) and pro-inflammatory cytokines that induce the expression of membrane receptors on the vascular endothelium and also the expression of ligands on leukocytes [5]. Leukocytes circulating in the blood vessel adhere to the endothelial wall in response to the presence of chemokines, proceeding to a rolling motion. Leukocytes become activated when their surface ligands bind to endothelium receptors. This activation causes the leukocyte to exit the blood vessel and go into the affected tissue to contend against the pathogen. This process is known as transendothelial migration or extravasation, illustrated in Figure 1.1.

The major biomarkers of an inflammatory process are TNF-α and IL-1, with their physiological effects including fever, blood vessel dilation and an increased permeability. Once the invading pathogen is removed, the inflammation must be stopped to prevent tissue damage. IL-10 is one of the main players in the anti-inflammatory response by downregulating cytokine expression. However, inflammatory processes that cannot be stopped or its source identified, can give rise to chronic inflammation, including Crohn's disease, asthma and tuberculosis [5].

Being able to measure the concentration of cytokines in a biological sample may provide useful information. For example, tuberculosis (TB) patients show elevated levels of INF-γ and tests have been developed for its diagnosis. In these tests, a blood sample is drawn from the patient and mixed with antigens from the bacteria that causes TB. White blood cells of an individual who has been exposed to the pathogen will secret high quantities of IFN-γ. A quantitative assay of this cytokine will determine if the patient is indeed infected with TB or not [13].

Furthermore, cytokine detection can help elucidate signaling mechanisms distorted in different pathologies. For instance, although some cytokines help in the removal of cancerous cells, these cells may benefit from other circulating cytokines

that induce cellular proliferation, adopting them as growth factors. In this case, knowledge of the intercellular signaling mediated by cytokines could help in the development of anti-tumor drugs and therapy evaluation [14].

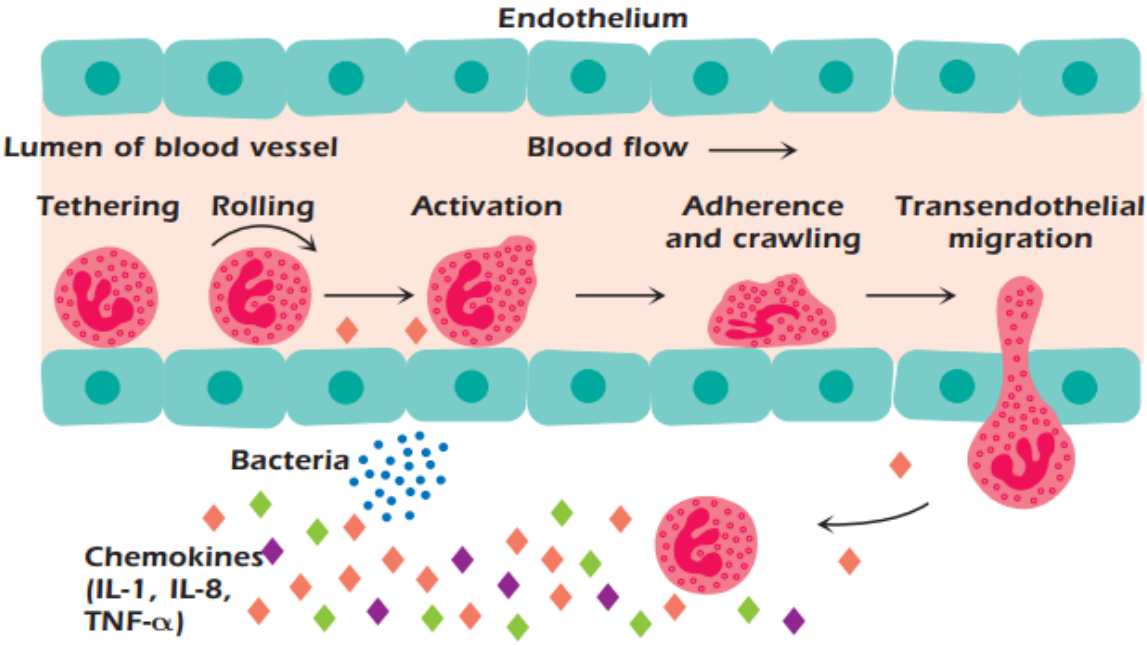

Figure 1.1: Schematic of the activation and extravasation of a leukocyte in response to cytokines. When bacteria enter a tissue, neighboring cells start secreting cytokines. These cytokines in turn, induce expression of membrane receptors in the vascular endothelium and their ligands on leukocytes. When the membrane receptors on the endothelium bind to the ligands on a leukocyte membrane, the leukocyte becomes activated. Activated white blood cells will undergo an adherence process and eventually migrate into the interstitial space, where they will contend against the bacteria present. Adapted from [5].

1.3 Cytokine quantification methods

There are two main methods by which cytokine secretion is assayed, both utilizing immunochemistry methods to selectively measure the protein of interest. These methods are:

1.3.1 Enzyme-linked immunosorbent assay

Also called ELISA, is the gold standard test for cytokine quantitation. This assay is typically conducted in 96-well plates. One variant of the assay uses antibodies immobilized on the bottom of each well which bind specifically to target molecules (analytes) contained in a sample. Detection antibodies (*i.e.* antibodies conjugated with reporter molecules) are then added to each well. The reporter molecule is usually an enzyme which will catalyze the conversion of a substrate to an optically readable product. Figure 1.2 shows a schematic representation of an ELISA test.

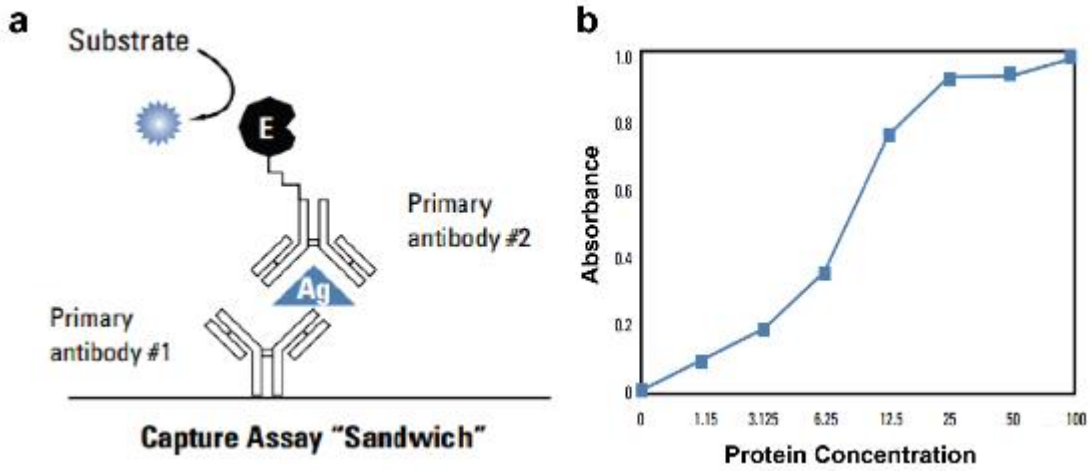

Figure 1.2: a) Representation of the molecular interactions that take place on a sandwich immunoassay. A capture antibody is immobilized on a surface which will specifically bind to the molecule of interest. A second antibody, conjugated to an enzyme, will bind to different epitopes of the biomolecule. The enzyme will catalyze the conversion of a substrate into an optically readable product. b) Typical graph obtained from an ELISA test, where the absorbance is plotted against a protein concentration. Adapted from [15].

ELISA is also called a sandwich immunoassay, since the analyte is sandwiched between two antibodies. Variations of this method include the use of microbeads fluorescently labeled with a barcode, where different beads are functionalized with capture antibodies for different proteins and deposited in the assay wells, this enables multiplexed quantification of cytokines. Although being a functional method and highly sensitive, it suffers from different drawbacks, such as long incubation times and multiple washing steps, making it tedious and repetitive. Furthermore, outcomes are strongly dependent on the skills of the individual performing the assay [16].

1.3.2 Flow cytometry coupled with intracellular staining

Another typical method for cytokine quantitation is flow cytometry coupled with intracellular staining. Here, cells are stimulated in the presence of a secretion inhibitor, then fixed and permeabilized, so fluorescently labeled antibodies may enter the cell and bind to the cytokines of interest. Cells are then passed through a laser by means of a fluidic system, the laser excites the fluorescent labels inside the cells causing them to emit light in a longer wave. Detectors are used to measure the light scattered by the antibodies. The emitted light brightness is correlated to the amount of analytes in each cell (Figure 1.3a) [17].

The main advantages of this technique are its high-throughput and its multiplexed quantification capabilities. In combination with the use of data mining algorithms and data visualization tools (*e.g.* viSNE), flow cytometry allows to generate a map of the different cells within a population. These data sometimes is used to associate an increase in cellular heterogeneity to a pathological state [18]. However, it also presents several disadvantages. Firstly, the proteins detected are intrinsic proteins (inside the cell), and its number may not compare with the actual amount that a cell will secrete in response to the same stimulus. Second, since the

cells are fixed, it is impossible to conduct further functional assays if needed. Finally, it only provides a snapshot image of a highly dynamic process.

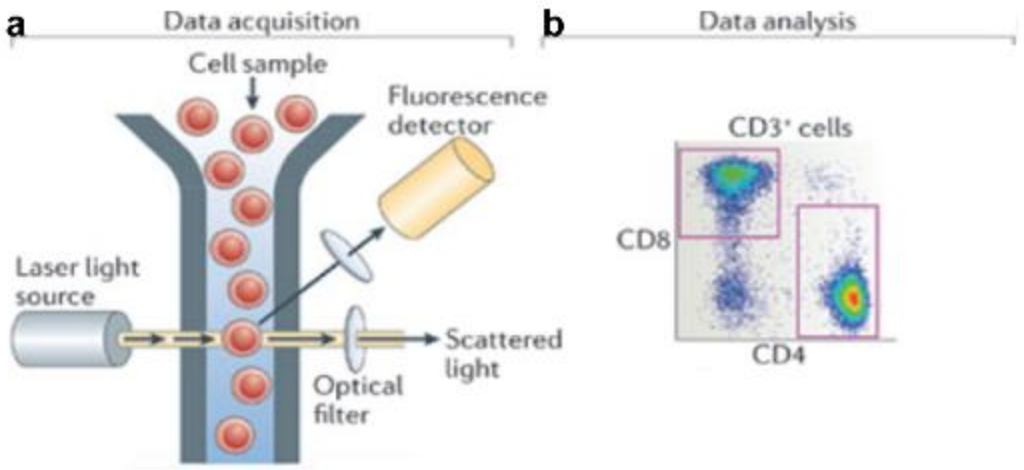

Figure 1.3: Flow cytometry coupled with intracellular staining. a) Cells previously stained with detection antibodies are passed through a laser. The detection antibodies will emit light in a characteristic wavelength; this signal is picked up by detectors that measure the intensity. b) Data visualization of the detected proteins. Adapted from [17].

1.4 Enter microfluidics

Microfluidic approaches have been reported that can overcome the limitations of methods currently used for cytokine quantitation. Microfluidics is the science and technology that deals with small volumes of liquids confined in a channel with dimension in the order of microns, where the behavior of the fluid is dominated by viscous forces, surface tension and fluidic resistance. These effects are exploited in a wide variety of applications [19]. One of the classic examples of microfluidic devices are pregnancy tests. These exploit the capillarity properties of paper in order to deliver hormones, present in the urine of pregnant women, to detection zones where antibodies are immobilized, providing an inexpensive method for biomolecule detection [20].

Sandwich immunoassays in microfluidic chips have already been demonstrated. One example is the work reported by Delamarche and collaborators, where they were able to quantitate TNF-α with picomolar sensitivity [21]. A polydimethylsiloxane (PDMS) block functionalized with capture antibodies was aligned to a chip that incorporated parallel microchannels. Recombinant protein was flowed through the channels at various concentrations. The chip was then peeled off and a new chip was placed perpendicularly over the patterned susbtrate; fluorescently labeled antibodies were then delivered through the block. The end result was a mosaic of fluorescence signals, shown in Figure 1.4. This method allowed to perform 170 assays with only 600 nL from a cell culture supernatant [21].

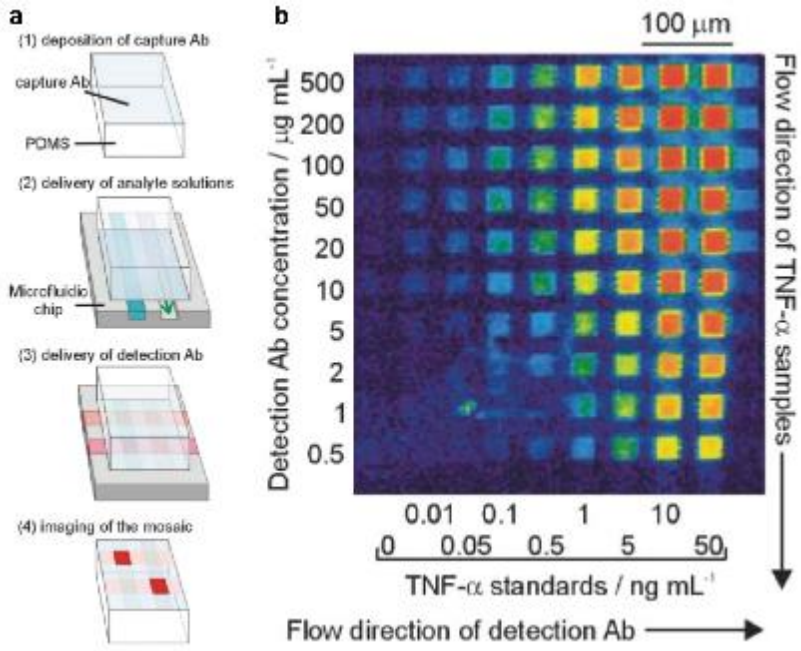

Figure1.4: a) Experimental workflow for microfluidic detection of TNF-α. Anti-TNF-α antibodies were immobilized in a block of PDMS and different concentrations of recombinant TNF-α were flowed, followed by a detection antibody delivery. b) Micrograph of the final result, showing that fluorescence intensity levels scale with both, concentration of detection antibodies and concentration of recombinant protein. Adapted from [21].

The fact that these kind of approaches utilize such small quantities of both, sample and regents, lowers the overall cost per assay and provides greater sensitivities and higher signal-to-noise ratios [22]. Furthermore, since the solutions are not pipetted but flow-driven into the chip, the test results do not rely on the operator's skills.

1.5 Integration capability

In order to devise new analytical methods that could help us get a better understanding about cytokine-mediated communication, it is necessary to integrate a biosensor next to a stimulated cell and monitor its secretory profile under different conditions in real-time. This level of integration is one of the main advantages that microfluidics offers, and has been the reason this field has been gaining interest. For example, Shirasaki and his collaborators reported a PDMS device consisting of microwells with capture antibodies functionalized at the bottom of each well (Figure 1.5a). Stimulated monocytes were trapped in an individual fashion in the wells where the media contained detection antibodies. Through the use of total internal reflection microscopy (TIRF) they were able to study in real time the release of IL-6. Furthermore, by also probing the plasma membrane integrity, they observed that the release of IL-1β occurs in bursts and it always occurs shortly after membrane permeabilization [23]. This behavior is illustrated in Figure 1.5b.

1.6 Problem definition

What Shirasaki and his team observed could have not been achieved with the typical methods of cytokine quantitation. They found that IL-1β does not follow the classical secretory pathway which involves traffic through the endoplasmic reticulum and the Golgi apparatus. In fact, various cytokines do not fallow this pathway and their own secretory pathways remain to be unveiled [24]. Therefore,

the motivation behind our work is to provide a platform for cytokine secretion quantitation that could help cellular biologists perform cell communication studies.

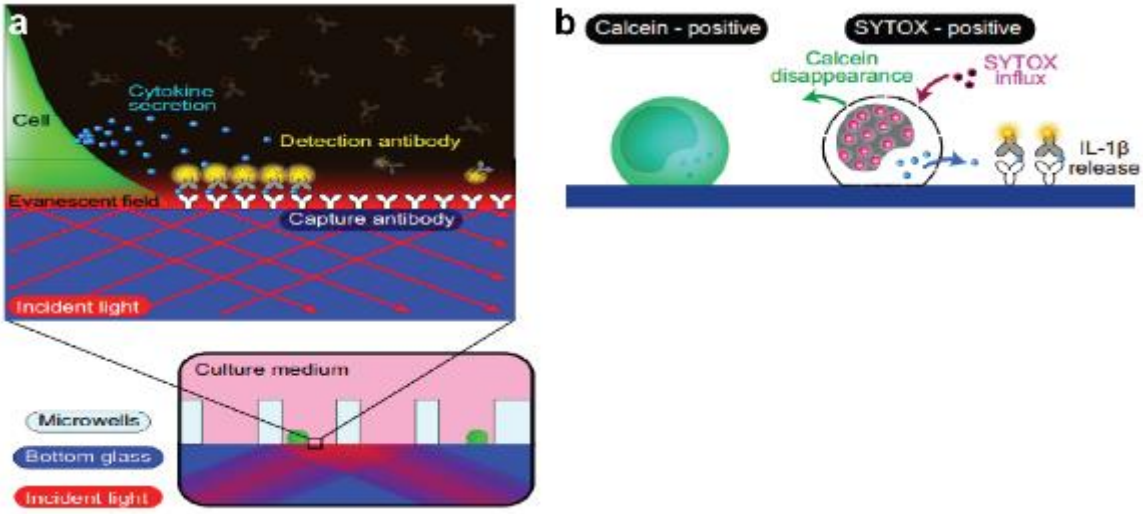

Figure 1.5: a) Single cells were seeded into microwells. Cytokine secretion was measured though fluorescently-labeled antibodies diluted in the medium. With the use of TIRF microscopy it is possible to observe only a small plane near the well bottom. b) It was observed that secretion of IL-1β always follows membrane permeabilization, shown by a loss in intracellular calcein signal and an influx of sytox dye. Adapted from [23].

2 Aim

The overall aim of this thesis is to design a microfluidic device capable of capturing a population of cells, subject them to different stimuli in a multiplexed fashion, and measure their secretory response. Our purpose is to provide a new analytical method for cell communication studies. In order to do so, we propose the following objectives:

To design and fabricate a microfluidic device. The final design integrates a biosensor, a cell capture mechanism, and a multiplexed on-chip stimuli delivery method.

When the microfluidic device is designed, the next step is its fabrication. This process involves the use of photolithography techniques for mold fabrication and soft-lithography techniques for mold replication.

When the microfluidic chip is assembled, its characterization follows. Among the parameters to characterize are the its final dimensions for both its layers and structures, and the proper performance of its elements. The final parameter to characterize is the effect of cell seeding time and cell concentration in the capture efficiency.

The final objective is to run a proof-of-concept assay to evaluate if our device can indeed be used to measure the release of communicating soluble factors from a population of cells captured in it.

3 Literature review

Many microfluidic devices have been described that are able to perform cell culturing. This implies the maintenance and growth of cells in the laboratory within a controlled environment. Polydimethylsiloxane (PDMS) is the material generally used for chip cell culturing. Some of the advantages offered by PDMMS are: biocompatibility, optical transparency, and its high porosity that allows oxygen to reach the culture chambers [25].

One example of a PDMS cell-culturing device is the one reported by the Quake laboratory. Their system contained 96 individually addressable culture chamber with volumes in the order of nanoliters (Figure 3.1). A great advantage of the device was its automation capabilities, making possible to automatically deliver fresh media in defined time intervals. Quake *et al* studied how long should human bone marrow stromal cells must be stimulated with osteogenic media to induce differentiation. Their results showed that the number of responsive cells scaled with the time of stimulation, but reached a maximum at ~96 hrs [26].

Yin and collaborators reported a device that incorporated a microfluidic gradient generator in series with cell culturing chambers. They tested the effect of 8 different concentrations of a biomolecule known for its nerve regeneration function on the proliferation rate of glial cells. They showed that the cells' response increases with concentration but reaches a maximum at ~1.78 ng/mL [27]. This device showed that several different cell culture conditions can be obtained in a microfluidic chip, with the maximum number of achievable conditions only limited by the array size of the culture chambers (Figure 3.2).

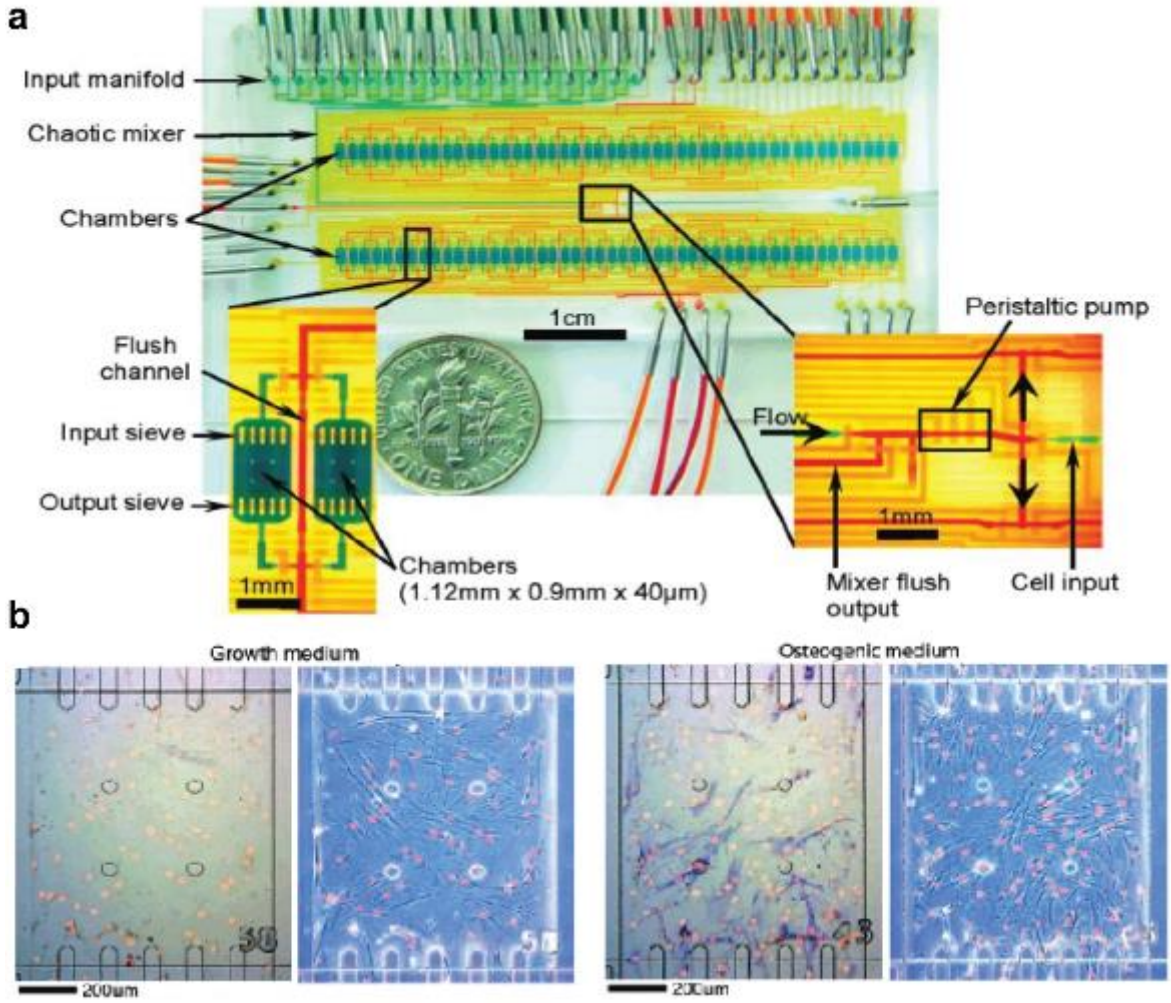

Figure 3.1: a) Device developed by Quake's group for cell culture. The chip contained 96 culture chambers, 16 inlets, a multiplexer for addressing each chamber, and peristaltic pumps for flow driving. b) Images in bright field and phase contrast showing the effect of regular growth medium and osteogenic medium in an osteoblast cell culture. Adapted from [26].

3.1 Cell patterning methods

It has been demonstrated that microfluidics devices are able to cultivate cells and stimulate them in a multiplexed fashion. Next, our attention will focus on the different

microfluidics methods for cell-trapping. The ability to generate well-defined and controlled arrangements of cells is useful for applications ranging from biosensor technology, tissue engineering, to cell biological studies. For example, cell-based studies might require that individual cells or cell populations, be accessed in a repeated manner to perturb them and evaluate their response, thus obtaining valuable information about cellular function and metabolism. Tissue engineering requires the placement of cells in specific locations in order to generate well-organized structures [28]. There are various techniques by which cells can be arranged and they entail either chemical or physical methods.

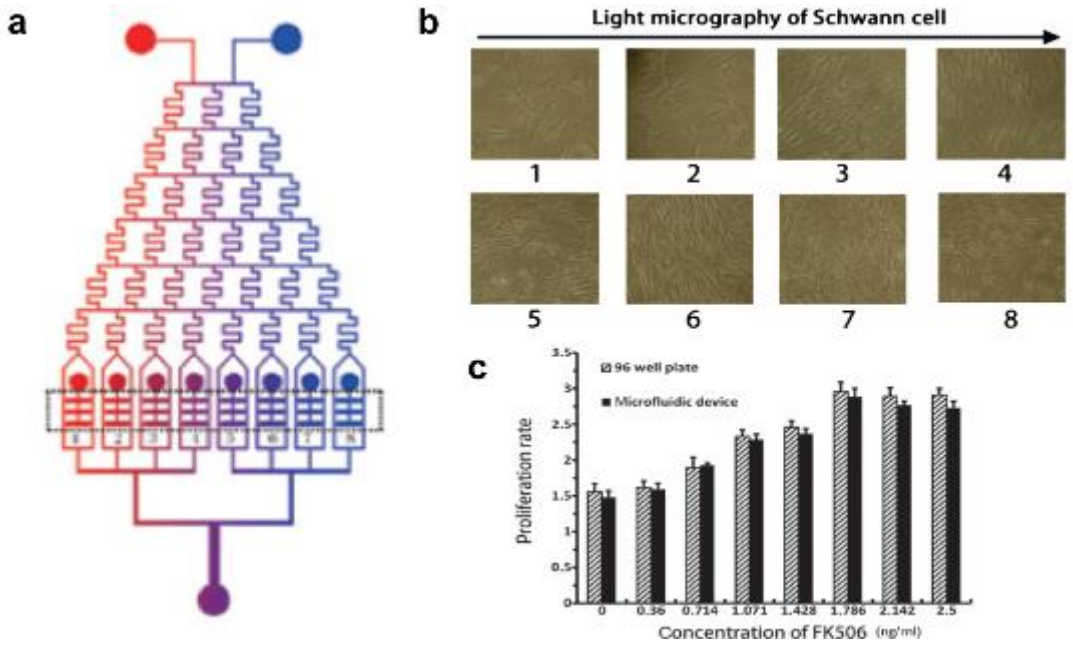

Figure 3.2: a) Microfluidic device that integrated a gradient generator in tandem with 8 cell culture chambers. b) Micrographs in bright field of a Schwann cell culture, showing that increased concentration of a nerve growth factor affected the proliferation rate. c) Results showed that proliferation rate scales with concentration nerve growth factor but reached a maximum at 1.786 ng/mL. Adapted from [27].

3.1.1 Chemical methods

The chemical methods to pattern cells exploit the phenomenon of adsorption, where molecules dissolved in a solution will form a layer of molecules on the substrate surface [29]. Surface modification or functionalization is the term employed when the properties of a surface (*e.g.* its hydrophilicity or hydrophobicity) are changed due to molecule adsorption [30].

There are two methods by which molecules can be specifically deposited on a surface using microfluidic techniques. The first method involves the placement of a polydimetylsiloxene (PDMS) block embedded with microchannels and placed on top of a substrate (Figure 3.3a). The solution with the molecules to be immobilized is then flowed through the microchannels. After a washing step, the PDMS block can be removed generating a pattern of molecules on the surface where the solution came in direct contact (*i.e.* the microchannels) [31].

The second method utilizes a PDMS microstamp (Figure 3.3b). The stamp is soaked with the solution containing the biomolecules that need to be immobilized, and then pressed against the substrate. The taller PDMS structures make direct contact against the surface, thus imprinting the molecules on it; the stamp is then removed leaving behind a pattern of biomolecules on the substrate [32].

Depending on the molecules that are used, the functionalized surface can either deter cellular attachment or promote it. For example, polyethylene glycol (PEG) has been shown to deter cell adhesion by repelling proteins due to its hydrophilicity, chain mobility, and lack of ionic charge [33]. On the other hand, molecules that are found in the extracellular matrix (ECM), such as fibrinogen and collagen, promote cell adhesion by binding to proteins that are present in the cell's membrane (*e.g.* integrins) [34]. Through the combination cell repelling molecules and cell adhesion promoters, Healy and his collaborators, demonstrated that

osteoblasts could be isolated in an individual manner by patterning vitronectin islands in a PEG polymer background. Furthermore, they also showed that they could influence cytoskeleton organization by modulating the size and shape of the adhesive islands (Figure 3.4) [35].

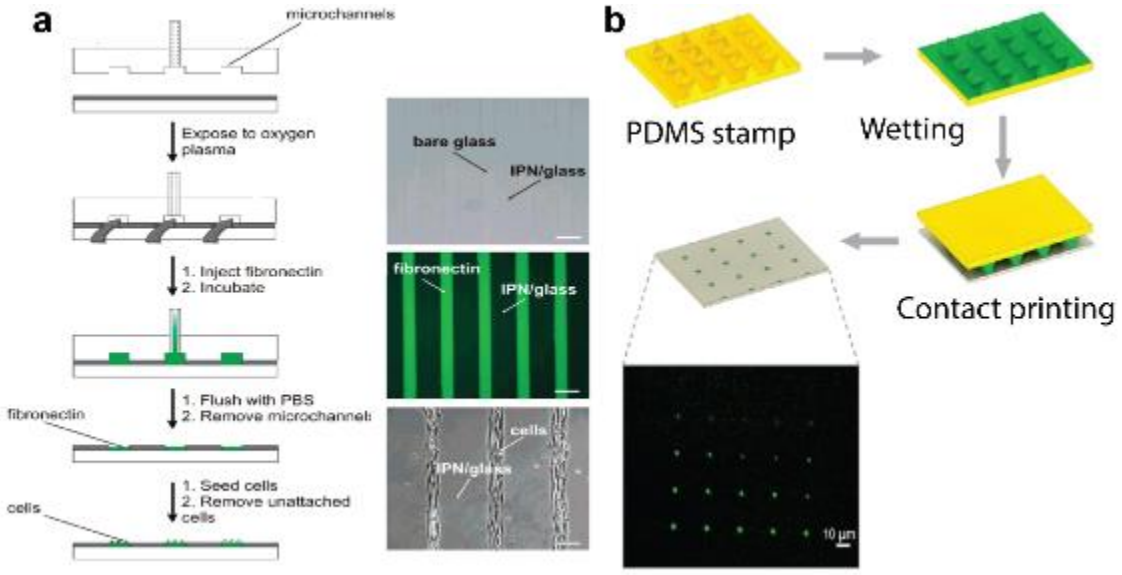

Figure 3.3: Molecular patterning using microfluidics. a) Patterning of fibronectin on glass with the use of microchannels. Modified from [31]. b) Patterning of fibronectin through the use of elastomeric stamps. With this approach a PDMS stamp is wetted with the solution containing the molecules to be immobilized. The stamp is then pressed against the substrate, leaving behind island where the molecules physisorbed. Adapted from [32].

Another biochemical method for cell patterning uses immobilized antibodies. These antibodies specifically recognize and bind to cell membrane markers. For example, blood cells have different proteins on their surface called clusters of differentiation (CD) that are utilized to identify and characterize the different types of blood cells [36]. Toner's research group developed a microfluidic device that

captured CD+4 T cells through immobilized anti-CD4 antibodies in a microfluidic channel. When whole blood was perfused into the device, T cells from HIV positive patients attached to the channel (Figure 3.5b). Cells were counted in order to monitor the disease progression and evaluate treatment options [37]. One of the major advantages of using this method is the ability to isolate or purify the cell type of interest from a heterogeneous cell population, such as blood.

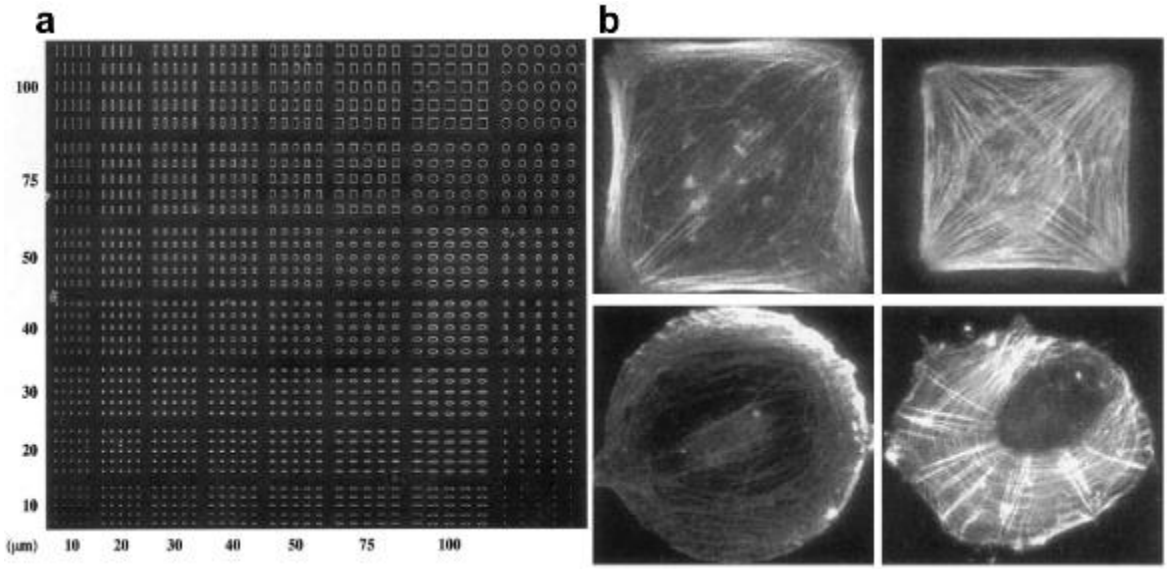

Figure 3.4: a) Photograph of the array of islands obtained by Healy et al. The array contained adhesive islands that varied in shape and size. b) Micrographs of individual cells in islands of different shapes, showing how these parameters affected cytoskeleton organization. Adapted from [35].

There are several advantages to using chemical methods for cell patterning. First, since soft-lithography techniques are used to generate the replicas for either the microchannels or microstamps, the fabricated molds can be used indefinitely. Second, by utilizing antibodies or aptamers (oligonucleotides that specifically bind to proteins [38]), a desired cell type can be captured without the need to isolate them in previous steps. However, certain limitations arise, for example, the structures of a microstamps can deform if enough pressure is applied against them, making the

printed features different from the original stamp features, ruining the desired cellular pattern. Furthermore, because the PDMS block has to be detached, proteins might dry, potentially losing their bioactivity [39]. Furthermore, since the solutions have to be incubated in order for the molecules to properly diffuse and attach to the substrate, the overall assay time increases.

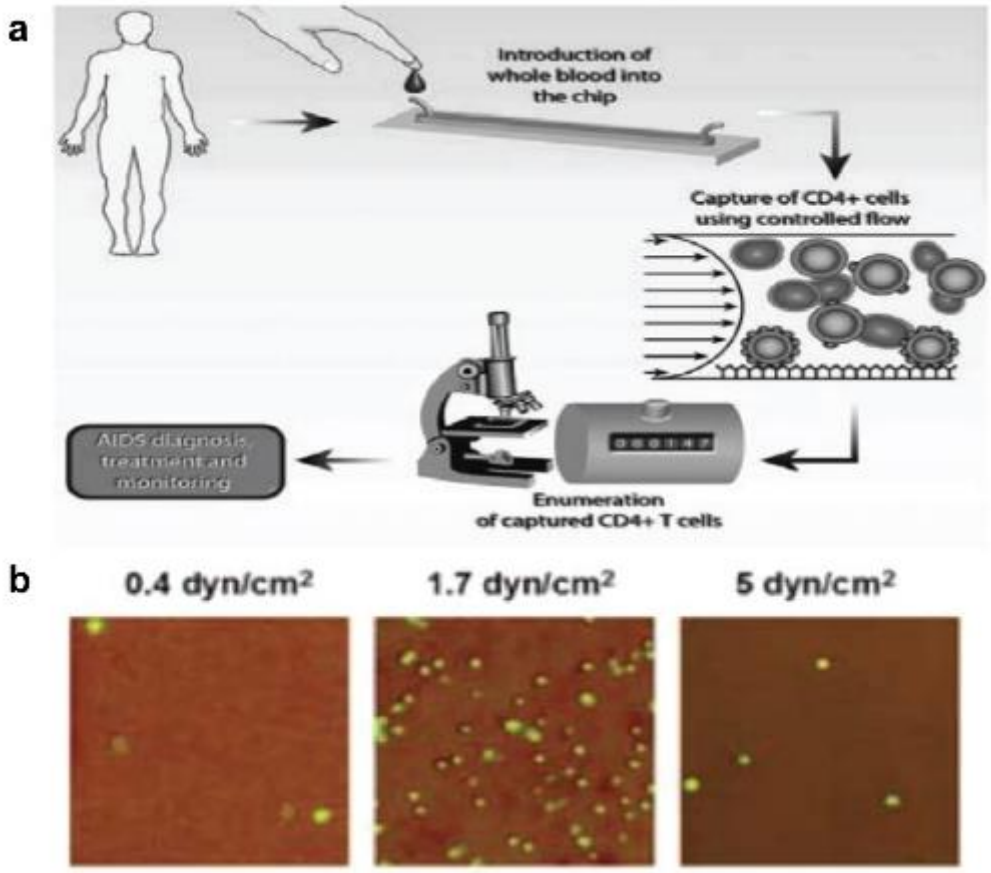

Figure 3.5: a) This device consisted of a single channel with immobilized anti-CD4 antibodies. The cells that were captured by the antibodies would then be counted; this count is useful in HIV diagnostics and treatment monitoring. b) Micrographs of cells stained with fluorescently labeled anti-CD4 antibodies captured in the chip, showing the effect of shear stress on the captured cells. Adapted from [37].

3.1.2 Physical methods

There are several physical methods through which cells can be patterned in a microfluidic device. The most straightforward method is to create an array of microwells at the bottom of a microfluidic channel. In general, a cell suspension is perfused into the channel, the flow is stopped once the channel fills with cells, the cells are then allowed to sediment into the wells, and excess cells are washed away. The Folch laboratory reported a PDMS device, replicated from a SU-8 master mold, that consisted of microwells arrayed in a hexagonal manner with varying diameters and depths. The maximum trapping efficiency that they achieved was 92% for basophilic leukemia cells and 85% for fibroblasts, with devices optimized in well size for each cell line (Figure 3.6) [40].

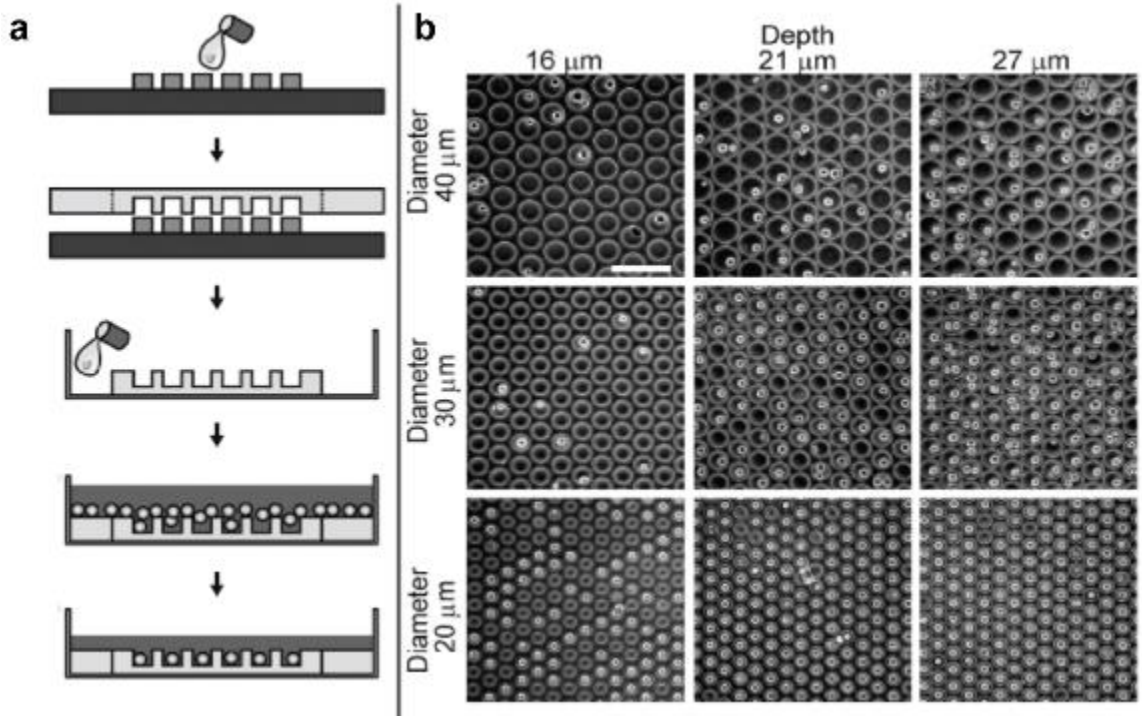

Figure 3.6: a) Process for obtaining the microwell device reported by Folch. Cells are seeded and allowed to sediment into the wells, while excess cells are then removed. b) Micrographs in phase contrast showing the effects of well diameter and depth in the efficiency of cell capture. Adapted from [40].

Other widely employed methods for cell trapping are hydrodynamic traps. These involve the placement of small channels inside a wider fluidic channel. These small channels give rise to weirs where cells can be trapped. One example consists of an array of structures suspended from the ceiling of the main channel; cells are dragged into the structure when flow passes through the small space left at the bottom. The top view of the structure is U-shaped ensuring the cells will not dislodge from the structure. DiCarlo observed up to 100 cells trapped in an area of ~1 mm^2 and about 85% of those cells remained in their trapping sites after 24 hrs (Figure 3.7) [41].

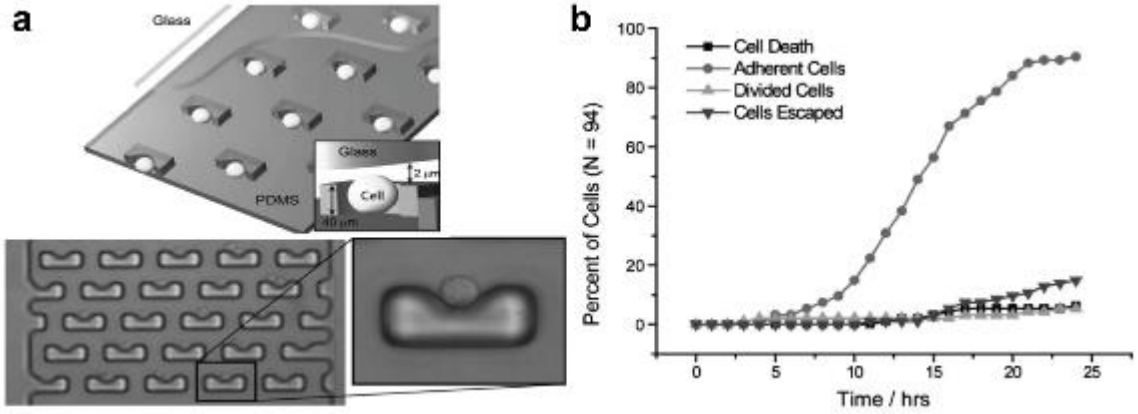

Figure 3.7: a). An array of hydrodynamic traps with a 2 μm gap between the traps and the glass slide. Fluid goes through the gap dragging cells into the trap. b) Plot showing the behavior of the trapped cells throughout culture time. After 24 hrs almost 100% of them adhered to the device, while only a 10% of trapped cell escaped form the traps. Adapted from [41].

Another type of hydrodynamic trapping involves a large serpentine channel. On each loop of the channel, cell trapping sites are created by small channels that connect that loop to the next one. A small flow will go through the small channel and cells will be dragged into them. Once the trapping site is occupied the flow diverts into the next site. Using this method, Kimmerling was able to isolate a single cell in

the first loop of a serpentine channel. As the cell divided, its progeny was captured in traps further down the channel [42].

Liu and collaborators reported a device that consisted of a c-shaped pneumatic structure that when actuated, raised a PDMS membrane into the microfluidic chamber, creating a reversible weir where cells could be captured (Figure 3.8a). They showed that it was possible to regulate the number of captured cells by optimizing several parameters, such as actuating pressure and seeding flow rate (Figure 3.8b) [43].

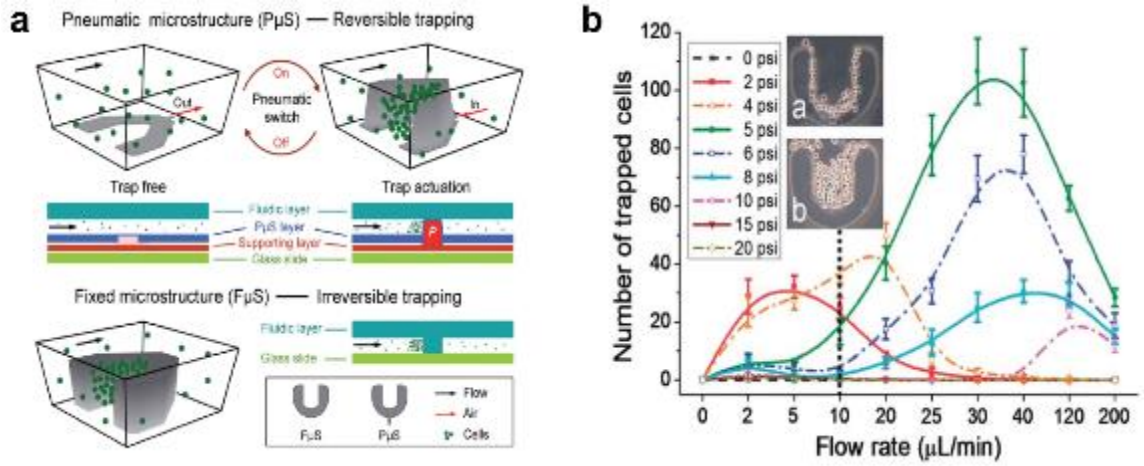

Figure 3.8: Reversible pneumatically actuated hydrodynamic traps. a) Schematic of the operating principle. b) Plots showing the number of trapped cells as a function of the flow rate and the actuated pressure. Adapted from [43].

Although the previously methods of cell patterning involve flow-driven methods, other more elaborated methods exist. These devices exploit different physical phenomena such as dielectrophoresis, optical tweezers and electromagnetic fields. In dielectrophoresis, electrodes placed in a microfluidic channel generate a non-uniform electric field, where they will exert a force on a dielectric particle (*e.g.* cell), either attracting it or repelling it to the electrode [44]. Optical tweezers involve the use of a highly focused laser. In the narrowest part of

the beam, a strong electric gradient is generated creating a dielectrophoretic effect on particles in its vicinity. The momentum of the incident photons is transmitted to the cell, enabling to move it at will (Figure 3.9a) [45]. A method that utilized electromagnetic effects has also been reported. In this method, the cell membrane is coated with magnetic microbeads; when the cells are flowed through a microfluidic channel, a magnetic field will attract the microbeads, which will drag the cells with them. One advantage of this method is that it is possible to purify a specific cell type from a heterogeneous mixture of cells by coating microbeads with membrane marker antibodies [46], bypassing the sample preparation step, which is a drawback of most microfluidic applications (Figure 3.9b).

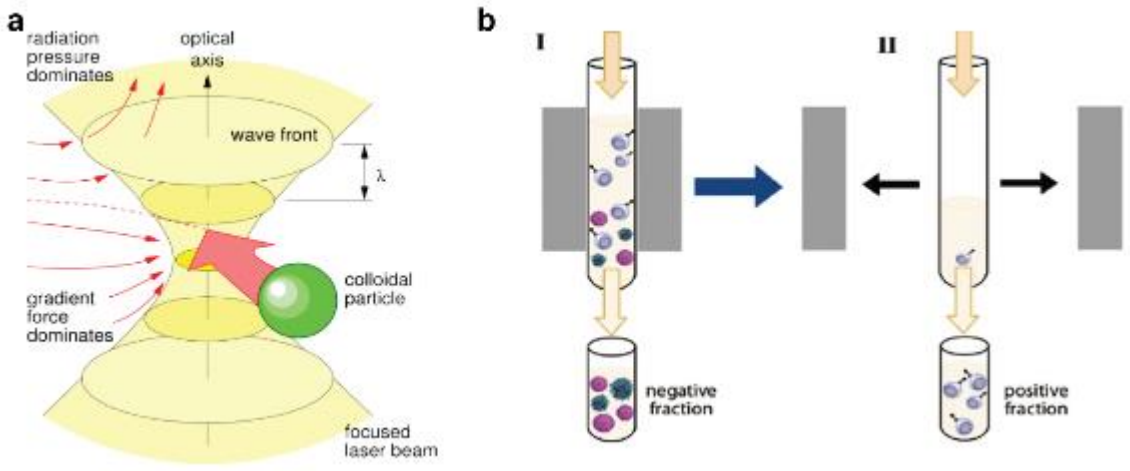

Figure 3.9: a) Working principle of optical tweezers. A highly focused laser generates an electrical gradient around its waist. This gradient induces an electrophoretic force, trapping dielectric particles in the vicinity. Taken from [47]. b) Cell isolation using magnetic beads. First, a cell suspension is passed through a column in the presence of a magnetic field, the beads are attracted to the magnets, dragging the cells with them and immobilizing them, while unwanted cells get eluted. After washing, trapped cells can be collected by removing the magnetic field. Adapted from [48].

3.2 Microfluidic-based cytokine biosensors

Several microfluidic devices have been reported that allow the detection of cytokines in a given sample. An interesting example is the device developed by Garcia-Cordero and Maerkl. This device made use of a circular membrane button to immobilize capture antibodies in order to perform a sandwich immunoassay in a PDMS chip. Through a process called mechanically induced trapping of molecular interactions (MITOMI), an actuation of positive pressure over the buttons pushes the membrane against the bottom of the microfluidic channel covering a defined area. By flowing a blocking solution through the chip, washing it, and then relieving the pressure in the buttons' channel line, unblocked spots are produced. Next, molecules are flowed, these form the scaffold of the immunocomplex but their formation is restricted to the unblocked areas. Furthermore, the size of the spot is regulated with the actuating pressure, increasing its contact area when higher pressures are used. In this way, up to three different antibodies were patterned under the button, forming concentric detection spots for IL-6, TNFα and IL-12 (Figure 3.10) [49]. Although the authors only demonstrated a proof-of-concept assay, they made it clear that this method could be incorporated in other devices, enabling a high-throughput immobilization of antibodies.

Many microfluidics devices have been conceived to detect proteins with high sensitivity in a particular sample; however, there have been only a few examples of microfluidic devices that integrate biosensing techniques in tandem with secretory cells. The devices created for this purpose, can either detect proteins secreted from single cells or from a cluster of cells. In the next sections, we will review some previous work regarding this integration.

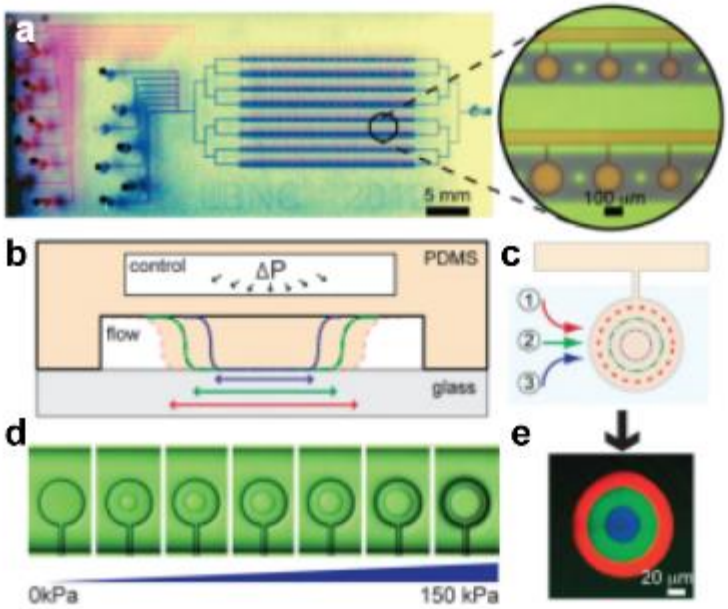

Figure 3.10. a) Microfluidic device with MITOMI buttons for high-throughput immobilization of antibodies. (b) An increase of pressure in the control line deflects a PDMS membrane which covers a defined area on a glass substrate. (c) As the pressure increases, a wider area is covered by the membrane. (d and e) By regulating the actuated pressure while flowing detection antibodies, concentric detection spots can be generated under the MITOMI button. Adapted from [49].

3.2.1 Single cell level

Microfluidic approaches are currently being develop to characterize the secretome profile of immune cells. Heath's laboratory developed a PDMS chip with a barcode array of antibodies immobilized in the surface, allowing the detection of twelve different cytokines secreted from individual cells trapped in chambers of ~1µL in volume. The device revealed highly coordinated secretory functions of monocytes when differentiated to macrophages; their results agreed with measurements obtained by flow cytometry [50].

Son and her collaborators developed a device with single cell trapping compartments that could be lifted by applying negative pressure. Their detection strategy used antibody-coated polystyrene microbeads, on which a sandwich immunoassay was performed. Detection antibodies were incubated along with the secretory cells, being able to detect secretion of INF-γ from stimulated T-cells [51]. This particular approach tries to compete with current TB diagnostic tests, and although they could only detect one cytokine per assay, the detection strategy can be multiplexed by employing fluorescently barcoded capture beads.

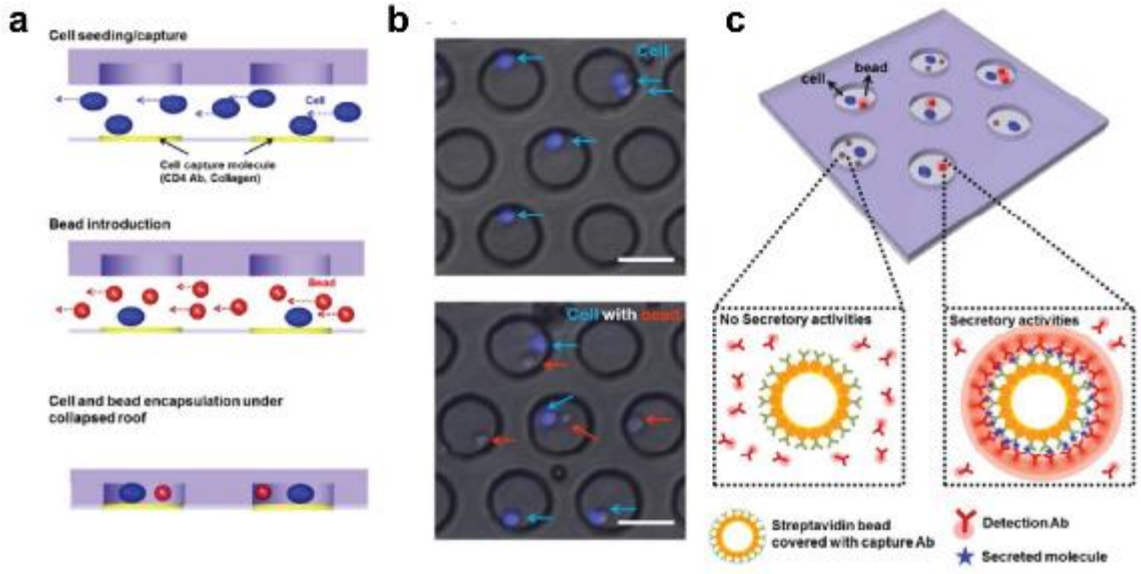

Figure 3.11: a) Cells are captured in assay chambers. Polystyrene beads with capture antibodies are then flowed through the device. Cells and beads are incubated in the assay chambers. b) Fluorescent micrographs of chambers with cells and beads. c) Secreted proteins bind to the beads, detection antibodies diluted in the medium will bind to the proteins immobilized on the bead surface, yielding a fluorescent signal. Adapted from [51]

3.2.2 Low-ensemble level

The devices mentioned in the previous section addressed the secretory profiling of single cells; however, the need to test populations of cells at the low-ensemble level remains unmet. This could help understand how a cellular population size affects the behavior and phenotypes of its own cells or cells from neighboring tissues. For example, cancer cells release pro-angiogenic paracrine regulators, while normal cells release anti-angiogenic regulators. Since cancer cells divide more rapidly than normal ones, the pro-angiogenic signal is increased, eventually leading to the formation of blood vessels around the tumor and having a direct effect on its proliferative rates and metastatic potential [52]. In this case, the information obtained regarding the size of a cellular population and its effect on the concentration of soluble factors could be useful in cancer research.

The Revzin laboratory has reported various microfluidic devices for paracrine signaling studies developing bio-interfaces for cell cultivation and protein sensing. One of their devices used immobilized anti-CD4 antibodies patterned around a gold electrode. This electrode was functionalized with aptamers which are oligonucleotides that specifically bind to analytes, similar to an antibody. When unbound, they adopt a hairpin configuration, but they suffer a conformational change when they recognize a protein. With the conjugation of a redox agent, this behavior is exploited to generate a change in the electrical current flowing through the sensing electrodes (Figure 3.12) [53]. With this approach, they were able to detect two different cytokines secreted from immobilized T cells. One advantage of aptamer-based biosensors is their ability to regenerate after a washing step with urea, opening the possibility to perform multiple assays using the same device [54]. One drawback of this approach is the need to perform two different surface functionalization steps, one for the antibodies and another one for the aptamers,

making the setup process elaborated. Moreover, patterning the gold electrodes needed for sensing complicates the fabrication process.

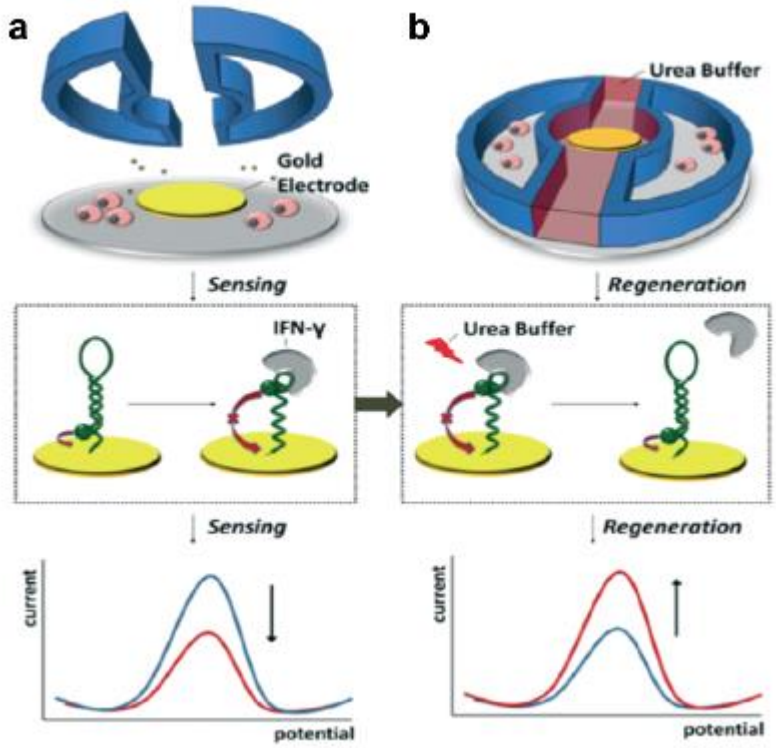

Figure 3.12: Schematic of a protein secretion assay using aptamers. A) Gold electrodes functionalized with the aptamers are place next to stimulated cells. When protein binds to the aptamers, these suffer a conformational change, inducing a signal suppression in an amperometric reading. b) Urea is flowed on the electrode, unbinding the aptamer and the protein, while cells are protected from the urea with pneumatically actuated walls. An amperometic reading shows an increase in signal due to the redox being closed to the electrode. Adapted from [54].

Another device reported by the Revzin laboratory utilized spotted antibody arrays on a glass slide, including anti-CD4, anti-TNFα, anti-IFNγ, and anti-IL10. Their chip consisted of collapsible assay chambers placed on top of the glass. Whole blood was perfused to the device and T-cells were captured by the anti-CD4

antibodies with a purity level of ~90%. These cells were then isolated in the assay chambers and their secretion levels measured through fluorescently-labeled detection antibodies (Figure 3.13) [55]. Their confinement in the small volumes produced a signal enhancement of 2-3 fold compared to unconfined cells.

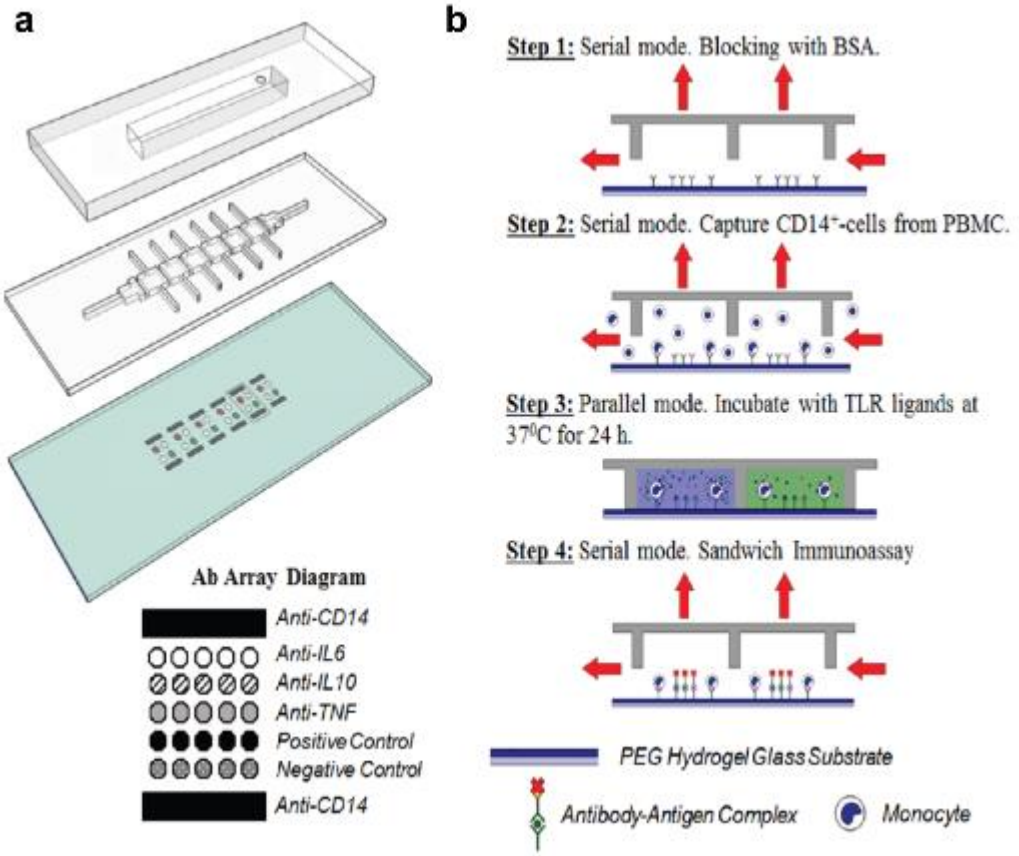

Figure 3.13: a) Device for detecting secreted proteins from a population of cells. The flow layer was composed of assay chambers, where the glass at the bottom was arrayed with different capture antibodies. b) Experimental workflow. The chamber walls were collapsed and cells were left to secrete their proteins. Finally, fluorescently labeled antibodies were flowed in the chip and measured. Adapted from [55].

3.3 Chapter summary

In this chapter a literature review was presented. First, we discussed current methods employed for cell patterning in microfluidic devices. These entail either chemical or physical methods for cell immobilization. The most straightforward method for cell capture involves the use of microwells, where cells are allowed to sediment. Other flow driven methods for cell capturing are easily implemented in microfluidic devices, such hydrodynamic traps. Furthermore, we discussed the microfluidic approaches that have been reported for protein quantification, where the MITOMI button shows a great ability to perform high-throughput antibody immobilization. Integrative approaches, were protein sensing strategies are placed next to secretory cells were also presented. These devices can either detect proteins secreted from single cells or small cell assembles.

4 Methods and Materials

In this chapter we discuss the methodology employed in order to achieve our aim. First, we provide an account of how the microfluidic device is designed and fabricated. Next, we describe how the experiments are performed for both the cell patterning method and the biosensing element, furthermore, we outline how the data is acquired and analyzed.

4.1 Chip Design

Our device follows an experimental workflow, in which cells are trapped (Figure 4.1a) and stimulated, the secreted proteins are allowed to diffuse into the detection zone (Figure 4.1b), and then detected by fluorescently labeled antibodies (Figure 4.1c). We selected the pneumatically actuated reversible hydrodynamic traps for cell capture, and a MITOMI button as the biosensing technique. Both elements make use of pneumatic structures which facilitates their integration in the same layer.

Furthermore, the ability to unactuate these structures is an advantage that can be exploited. The cell trap can be unactuated after cell loading, allowing the free diffusion of proteins into the sensing area, in contrast to static hydrodynamic traps, that do not permit this. The MITOMI button when actuated will cover a defined area on the glass slide, such that when a blocking solution is delivered to the chip and washed, the area will remain unblocked. The MITOMI button will then be unactuated and the unblocked area will be used to immobilize capture antibodies through physisorption. After the antibodies are immobilized on the surface below the MITOMI button, this is actuated to protect the antibodies during the cell loading step. This will inhibit proteins from the culture media to bind and saturate the detection zones due to flow conditions. Once the cells are stimulated, the button can then be unactuated so that secreted proteins bind to the capture antibodies. At the end of

the assay, the detection spot can be protected once more when detections antibodies are flowed in through the chip, minimizing cross chamber communication.

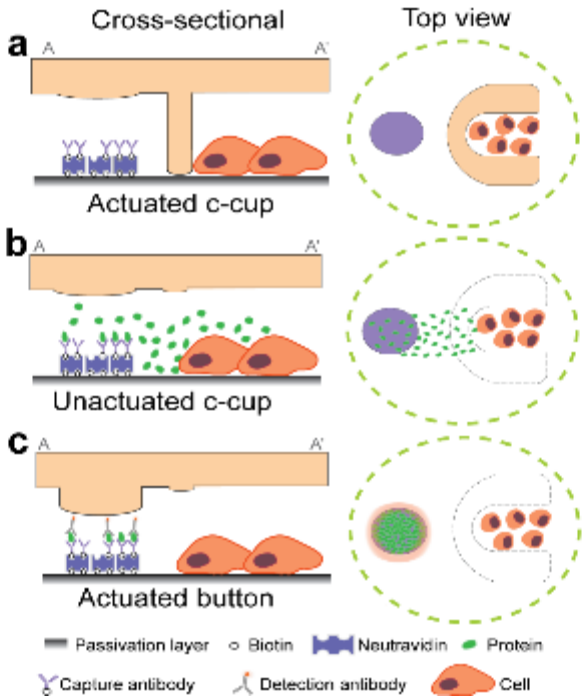

Figure 4.1: Proposed experimental workflow. a) The trapping mechanism is actuated in order to capture a cell population. b) Cells are stimulated and their secreted proteins are able to freely diffuse into the sensing spot. c) Detection antibodies are then added to detect the proteins in the sensing area.

The device consists of two layers: a flow layer with the assay chambers and microfluidic channels, and a control layer with all the pneumatic structures. The flow layer consists of a 4 x 16 array of circular chambers of 1200-µm diameter, with 2275 µm of separation on the *x* axis and 1500 µm separation on the *y* axis (Figure 4.2). The 4 rows in the array attach to 8 inlets, and a purge outlet on one end and a single outlet on the other end. The 16 columns were divided in subsections of 4, each subsection connected to a single inlet and outlet, thus enabling up to four different

stimuli conditions for each experiment in a total of 16 chambers, providing enough data for statistical analysis. All the flow channels were designed with a 150 µm width.

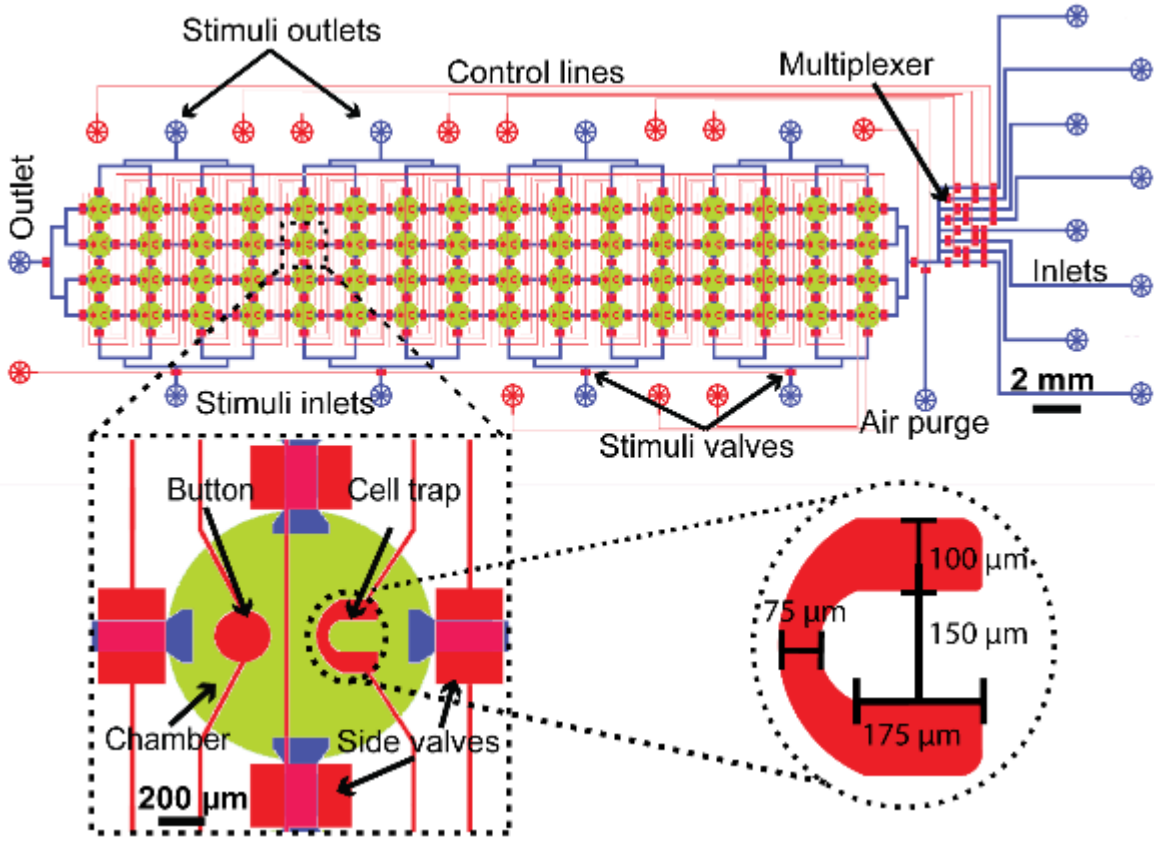

Figure 4.2: Chip design and close-up to an individual chamber showing the constituent parts. The control layer is shown in red, the flow layer in blue, and assay chambers in green. A close-up to the c-cups show the final dimensions of the structures.

The control layer design integrates a 4 x 16 array, that matches that of the chambers in the flow layer, with structures that include four side valves, to inhibit cross chamber communication. The MITOMI button for protein secretion detection has a diameter of 180 µm. A c-cup for cell patterning, designed with a posterior width of 75 µm, side which is narrower than the top and bottom portions, which measure 100 µm. The intention behind this design is to create a structure that

deflects more easily from the sides than the back. As a result, when pressure is applied, the back portion will create a weir structure where cells dragged by the fluid flow will be captured. Meanwhile, the top and bottom portions will generate walls at the same actuating pressure, preventing cell dislodgement from the traps. In addition to the structures previously mentioned, the control layer also incorporates a valve-based multiplexer for inflow reagent selection, and valves for air-purging and for stimuli delivery, all measuring 450 x 300 µm

4.2 Chip fabrication

The devices were fabricated using standard photolithography and soft lithography techniques. In general, the process scheme for obtaining a microfluidic device by soft lithography consists of two processes, illustrated in Figure 4.3. First, the master mold is fabricated by depositing photoresist on a silicon wafer, exposing the desired pattern with UV light, and developing it. Next polydimethylsiloxane (PDMS) replicas are manufactured and bonded to glass slides.

4.2.1 Mold fabrication

The mold was fabricated using photolithography techniques, with each mold fabricated separately and using different protocols. The control layer mold was fabricated using SU-8 negative photoresist, yielding rectangle-shaped profile structures. The flow layer mold was made using a combination of SU-8 photoresist (for assay chamber) and AZ photoresist (for the microfluidic channel). The positive photoresist structures will adopt a semicircular profile after a reflow process, to ensure proper valve sealing. For both layers, a new silicon wafer (Desert Silicon Inc.) was cleaned in an oxygen plasma machine (Zepto, Diener Electronic GmbH & Co. KG) for 10 min. After this process, the wafer was placed on a spin coater (SCS 6800 Spin Coater Series, Specialty Coating Systems, Inc.) and GM1060 (Gersteltec Sarl) photoresist dispensed on top of it. The spin-coating process was carried out at 1000

rpm for 40 sec with acceleration and deceleration ramps of 100 rpm/s, expecting to obtain a 25-μm height layer. This is followed by a relaxation time of 1 hr which permits the coated photoresist to level out across the wafer. Next, a process called soft-bake follows, which consists of evaporating the remaining solvents in the photoresist in order to prevent N_2 bubble formation during exposure and also to improve resist adhesion to the substrate. The soft-bake step was performed on a hot-plate (PC-420D, Corning Inc.) at 65°C for 10 min and at 95°C for 20 min starting from 50°C and increasing 5°C every two min until reaching the required 65°C and 95°C soft-bake temperatures.

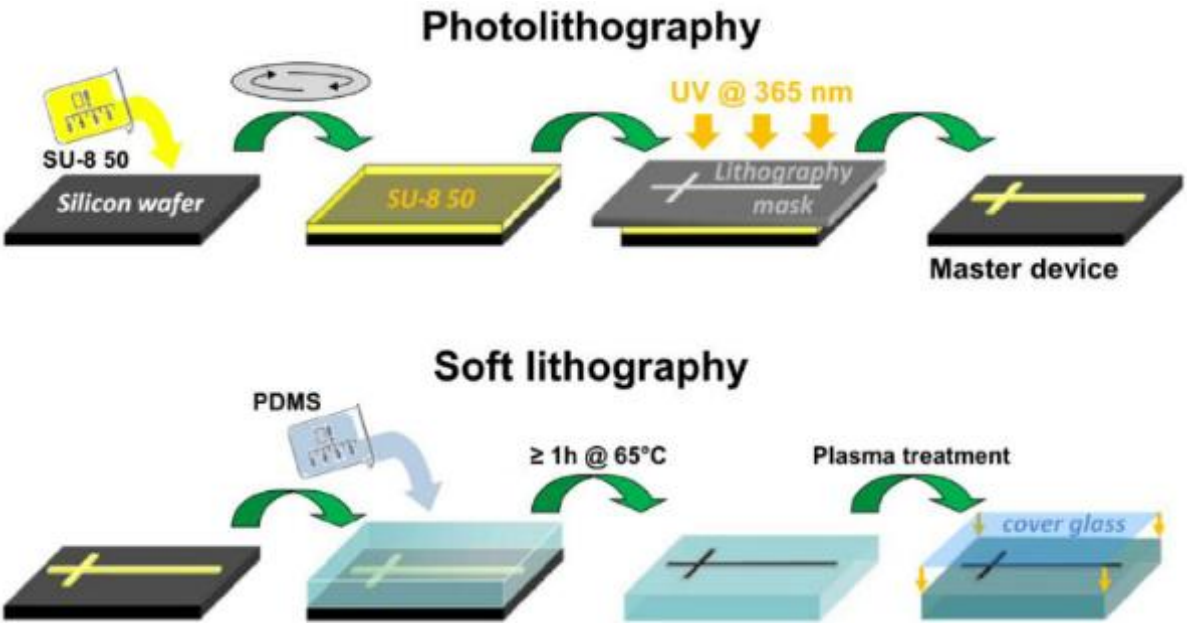

Figure 4.3: Chip fabrication process schematic. The photolithography method is done by depositing resin on a silicon wafer, spin coat it, exposing to UV light under a mask with the desired pattern and developing. The soft lithography process consists of pouring PDMS on the master mold, curing, peeling off and plasma bonding the PDMS chip to a glass slide. Taken from [56].

The wafer is then placed in a micropattern generator (µPG 101, Heidelberg Instruments Inc.) onto which the design of the layer is uploaded. The generator lets UV light from a 70 mW laser expose the SU-8 deposited on the wafer, initiating the cross-linking through activation of the photoactive component. A post-bake was performed that accelerates the cross-linking and makes the exposed areas insoluble in a developer. The process started at 50°C and increased 5°C every 2 min, holding it at 65°C for 10 min and for 20 min at 95°C.

The development of the photoresist was performed by bathing the wafer with propylene-glycol-monomethyl-ether-acetate (PGMEA) (484431, Sigma-Aldrich Co.) for ~15 sec, followed by an isopropanol (W292907, Sigma-Aldrich Co.) rinsed with water, and repeating these steps until the unexposed resin was washed away completely. The wafer was left to air dry and then subjected to a hard bake at 230°C in a convection oven (UF55, Memmert GmbH). This reduces cracks and improves attachment between the structures and the wafer.

For the flow layer mold, once the assay chamber structures were fabricated, the wafer was subjected to a plasma treatment for 90 sec, rendering its surface hydrophilic. After this, the wafer was spin coated with an adhesion promoter (Gersteltec Sarl, Pully) at 3000 rpm for 20 sec, then placed on the hot plate at 120°C for 5 min. The wafer was then coated with AZ9260 positive photoresist (Microchemicals GmbH), first at 500 rpm for 10 sec, to spread the photoresist all over the wafer, followed by 1800 rpm for 40 sec with acceleration and deceleration of 1000 rpm/s, expecting to yield a layer about 10-µm height. A two-step pre-bake at 95°C for 1 min and 120°C for 3 min is performed, followed by a second spin-coating with the intention to obtain a final layer of about 20-µm height. A second pre-bake was done at 95°C and 120°C for 1 and 6 min, respectively. During the pre-bake, water in the photoresist evaporates. However, water is needed to provide a uniform developing rate, for this purpose the wafer is rehydrated. In the rehydration

step, water from the air diffuses into the photoresist, if not enough time is given for the resist to fully hydrate, the resist at the bottom will have a lower water concentration than the top portion. In this case, the top photoresist will have a higher development rate than the bottom, yielding structures with an overcut profile [57]. For the photoresist thickness used in our mold, 1 hr of rehydration ensures proper photoresist hydration and an equal development rate, thus improving the profile of the structures.

The negative image of the flow layer design was uploaded into the micropattern generator. This negative image is the inversion of the layer, that is to say, the white areas of the design (where light should incise) are turned dark, and viceversa. The reason behind the use of the negative image, is that positive photoresist becomes more soluble in a developer when exposed to UV light. Therefore, light should incise only on the spaces where there will be no structures patterned. The design is then aligned to the wafer through the localization of alignment marks, patterned along with the assay chambers. The offset and rotation angle was obtained and a single exposure at 60mW at a 60% intensity was performed. The UV light exposure renders the photoresist soluble to the developer. The development was performed by bathing the exposed wafer in a 1:4 v/v dilution of AZ400K (Clariant Corporation AZ Electronic Materials) developer in distilled water for ~3 min, rinsed with distilled water, and repeating until all exposed resin was washed away completely. To ensure proper valve closing of the flow channels, these must adopt a semicircular profile (Figure 4.4). In consequence, the AZ photoresist was subjected to a reflow process on a hot-plate at 130°C for 5 min. This temperature is near the photoresist glass transition, causing the photoresist to melt. When melted, the resist adopts a round shaped profile due to surface tension effects and the surface properties of the wafer.

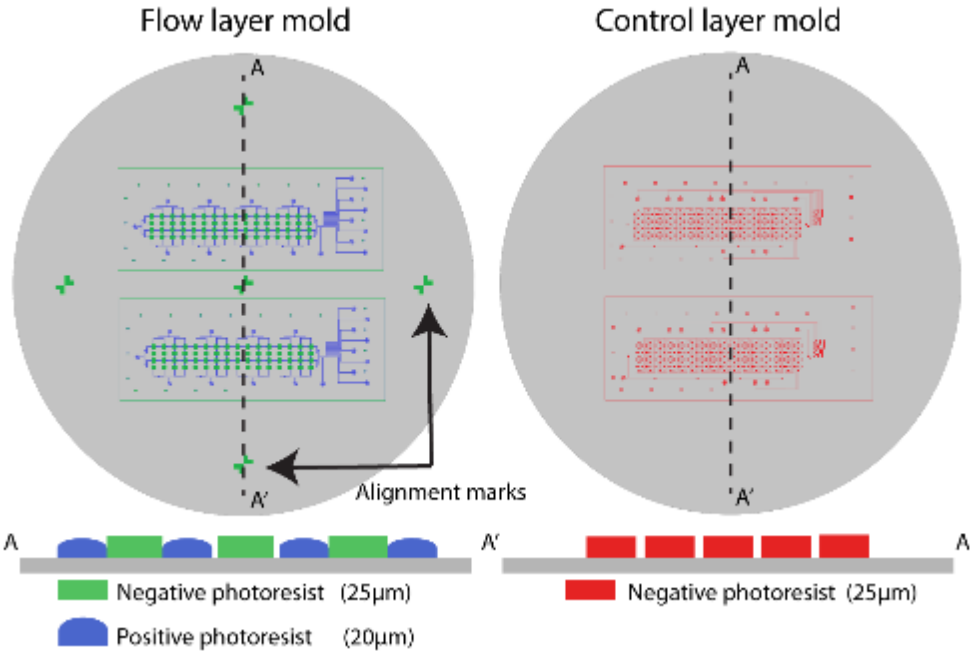

Figure 4.4: Schematic of the molds fabricated. The flow layer control mold was made by first patterning a layer of negative photoresist. This layer included the assay chambers and alignment marks for further photoresist patterning. The second layer consisted of positive photoresist for the patterning of microchannels. This photoresist adopted a semicircular profile after a reflow step. The control layer mold consisted of a single layer of negative photoresist, where all the control structures were patterned.

4.2.2 PDMS chip fabrication

The PDMS chip manufacturing started by treating the master molds with trichloromethylsilane (679208, Sigma-Aldrich Co.) through evaporation deposition for 2 hrs, thus rendering the molds hydrophobic. Next, for the control layer manufacturing, a 5:1 w:w PDMS pre-polymer to curing agent ratio (Sylgard® 184 silicone elastomer kit, Dow Corning Corporation) was mixed in a planetary centrifugal mixer (AR-100, Thinky USA Inc.), poured on top of the control-layer mold,

placed in a petri-dish. The petri dish was then introduced to a vacuum chamber for degassing over a period of 10 min.

For the flow layer, a 20:1 w/w ratio of PDMS pre-polymer to curing agent mix was homogenized in the planetary centrifugal mixer, then spin-coated onto the mold at 1580 rpm for 40 sec, with an acceleration and deceleration of 1000 rpm/s. Both molds were then introduced to a convection oven and left to cure at 80°C for 29 min. After this time, the control layers were cut with a hooked blade scalpel, peeled off the mold and the inlet holes punched (MP10-UNV, SCHMIDT Technology Corporation). The control layer was manually aligned on top of the flow layer under a stereomicroscope (Stemi DV4, Carl Zeiss Microscopy GmbH). To bond the two layers, the assembled device was entered in the oven at 80°C for 90 min, enabling a proper bond between them. The chips were then cut with a straight scalpel, and flow channel inlets and outlets punched.

The PDMS chips and a glass slide were placed upside down in the plasma treatment machine for 90 sec. The chips are then flipped over and rested on top of the treated side of the glass slide, trying to avoid air bubble formation. Finally, the devices are placed on a hotplate at 90°C for 5 min to ensure proper bonding. This process is shown in Figure 4.5.

4.3 Chip preparation

Glass slides were washed with milli-Q water (EMD Millipore, Merck KGaA) and a detergent in a sonicator bath for 30 min. The water was then replaced with clean milli-Q and sonicated again for 30 min. Water was then replaced once more and the clean glass slides were stored in it until being used with the PDMS chips.

After the PDMS chips were bonded to the glass slides, Tygon tubes (Tygon® AAD04103 Microbore Tubing, Saint-Gobain PPL Corp.) were filled with milli-Q water

and connected to the control layer inlets. The tubes on the other end were connected to a custom-made pressure control panel (Figure 4.6), containing solenoid valves (MH1-A-12VDC miniature valves, Festo) controlled by a LabVIEW interface (2015 Student Edition, National Instruments), which could switch a pneumatic line pressurized at 24 psi.

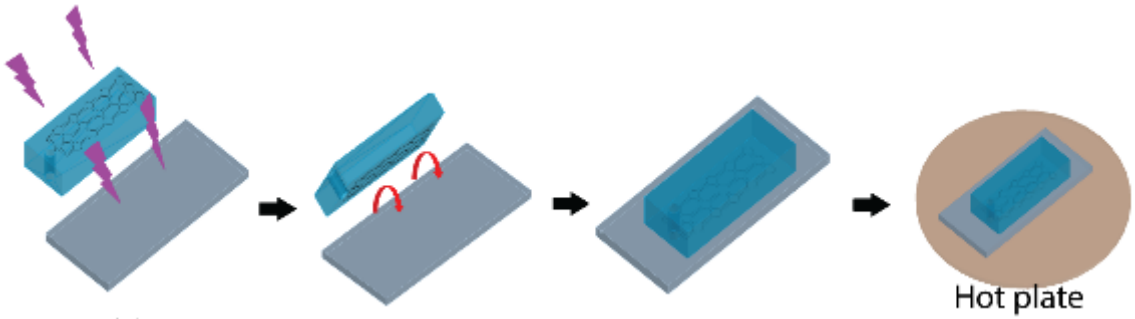

Figure 4.5: Schematic of the PDMS-glass bonding. The bottom side of the chip and a glass slide are plasma treated. Next, the treated side of the PDMS chip is placed on top of the treated side of the glass slide. Finally, the assembled device is positioned on a hot plate.

First, all the pressure lines are activated for 5 min to ensure proper filling of the control channels. After this step, only the necessary lines are left pressurized (typically the multiplexer valves and side valves that isolate the assay chambers) while the remaining lines are depressurized. Phosphate buffered saline 1x (PBS) (P5493, Sigma-Aldrich Co.) is then injected to the device at 2.5 psi for 20 sec. The common outlet is blocked for a period of 5 min. The purpose of this step is to hydrate the assay chamber and flow channels, and also to eliminate remaining air pockets. The chip is then ready to be used in an experiment.

From this point on, unless stated otherwise, all solutions or suspensions utilized in the flow layer were injected at 2.5 psi, which generated a volumetric flow of ~6.666 µL/min (obtained from observing that 200 µL were consumed after 30 min

of perfusion at this pressure). The c-cup pressure line was regulated down to 21 psi, while the remaining control channels were maintained at 24 psi.

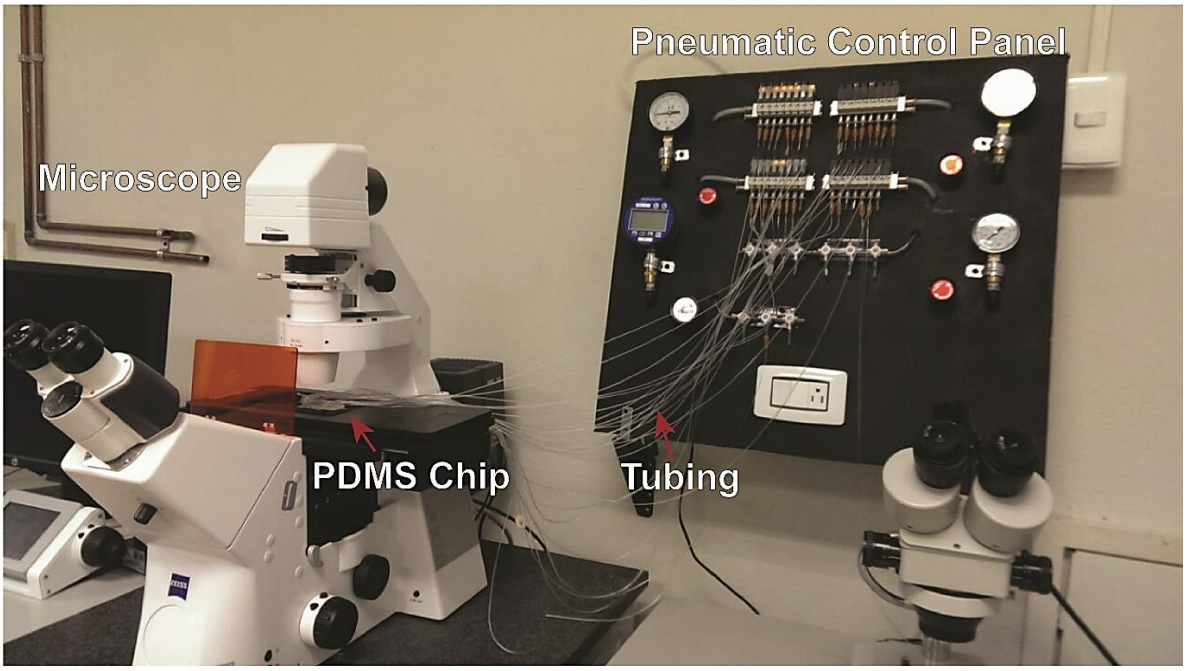

Figure 4.6: Experiment setup in the microscope workstation. The microscope is placed next to a pneumatic control panel. The chip is mounted on the microscope's stage and connected to the control panel via medical grade tubing.

4.4 Cell patterning experiments

We first characterized the mechanically induced trapping of cells. For this, a non-adherent cell line was cultivated in the laboratory and used to prepare four cellular suspensions of different cellular concentrations. These suspensions were injected to the chips for 30 min, and photographs were acquired every two min, measuring the number of trapped cells as a function of both cell concentration and seeding time.

4.4.1 Cell culturing

Monocytes from the THP-1 cell line were donated by Dr. Gertrud Lund (Cinvestav-Irapuato) and cultivated. The reason for utilizing a cell line is the advantages that it offers, primarily being cost effective and easy to use. Furthermore, since the cell line is immortalized, the cells proliferate in culture conditions, providing an unlimited supply of samples for conducting experiments [58]. Monocytes were selected because they secrete large amounts of tumor necrosis factor (TNF) when stimulated with lipopolysaccharides (LPS) [59]. This behavior can be exploited in future experiments, where proof-of-concept assays involving protein secretion quantification from a stimulated cell population, may provide further chip performance information.

4.4.2 Cell thawing

The cells were delivered frozen in 1mL vials and kept at -80°C until used. The cell thawing process was performed by gently agitating the vials in a water bath at 37°C, and immediately transferring the cell suspension to 15 mL centrifuge tubes, loaded with 6 mL of pre-warmed growth medium and centrifuged at 1500 rpm for 5 min with the intention of removing dead cells debris. The tubes were decanted and the pellets re-suspended in 1 mL growth medium, then transferred to T25 culture flasks with 7 mL pre-warmed growth medium, where they were incubated (MIDI 40, Thermo Fisher Scientific Inc.) at 37°C and 5%CO_2. Growth medium was completely replaced 24 hrs after thawing, and again every 2-3 days.

4.4.3 Culture medium preparation

THP-1 cells were grown in RPMI 1640 medium (21870, Gibco, Thermo Fisher Scientific Inc.) supplemented with 10% fetal bovine serum (FBS) (16000 Gibco, Thermo Fisher Scientific Inc.), 4.5 mg/mL glucose (G6918, Sigma-Aldrich Co.), 2mM

glutamate (35050, Gibco, Thermo Fisher Scientific Inc.), 10mM HEPES (15630, Gibco, Thermo Fisher Scientific Inc.), 1mM sodium pyruvate (11360, Gibco, Thermo Fisher Scientific Inc.) and 50 µg/mL penicillin-streptomycin (pen-strep) (15140, Gibco, Thermo Fisher Scientific Inc.). The glucose and pen-strep solutions were collected from the bottles with sterile needles and 5 mL syringes, and then passed through a filter (723-2520, EMD Millipore, Merck KGaA) before being dissolved in the growth medium.

The fetal bovine serum was first subjected to a water bath at 60°C for 1 hr to inactivate it, then the supernatant was suctioned with a 20 mL serological pipette and dissolved in the growth medium. All the solutions were prepared in a laminar flow hood (Purifier Logic+ Class II, Type A2 Biosafety Cabinet, Labconco,) to prevent fungal and bacterial contamination. The supplemented medium was stored at 4°C in 50 mL falcon tubes until used.

4.4.4 Sub-culturing

Once the cells reached 80% confluency, they were detached from the flask by suctioning the cell suspension and pouring it all across the bottom of the culture flask for three times. No trypsin treatment was needed because the monocytes are non-adherent cells. After this, 1 mL of the cell suspension was transferred into a new T25 flask loaded with 6 mL of fresh growth medium. Cells were then kept at 37°C and 5% CO_2 until reaching confluency again (typically 3-4 days). The remaining cellular suspension was used to perform the cell capture experiments.

4.4.5 Cell suspension preparation

10 µL of cell suspension that remained from passage were mixed with 90 µL of trypan blue. 10 µL of the resulting suspension are loaded in each chamber of a hemocytometer. The cells in two sets of 16 counting squares in the hemocytometer

(Figure 4.7) are counted with an inverted microscope (Axio Observer A1, Carl Zeiss Microscopy GmbH) under a 10x objective. The cell concentration is obtained by means of the following equation:

$$Cell\ concentration\ \left[\frac{cells}{mL}\right] = mean\ cell\ count * 10 * 10^4 \quad (4.1)$$

where 10 is the dilution factor of the cell suspension and 10^4 is the conversion factor from 0.1 µL, which is the volume of each set of counting squares, to 1 mL.

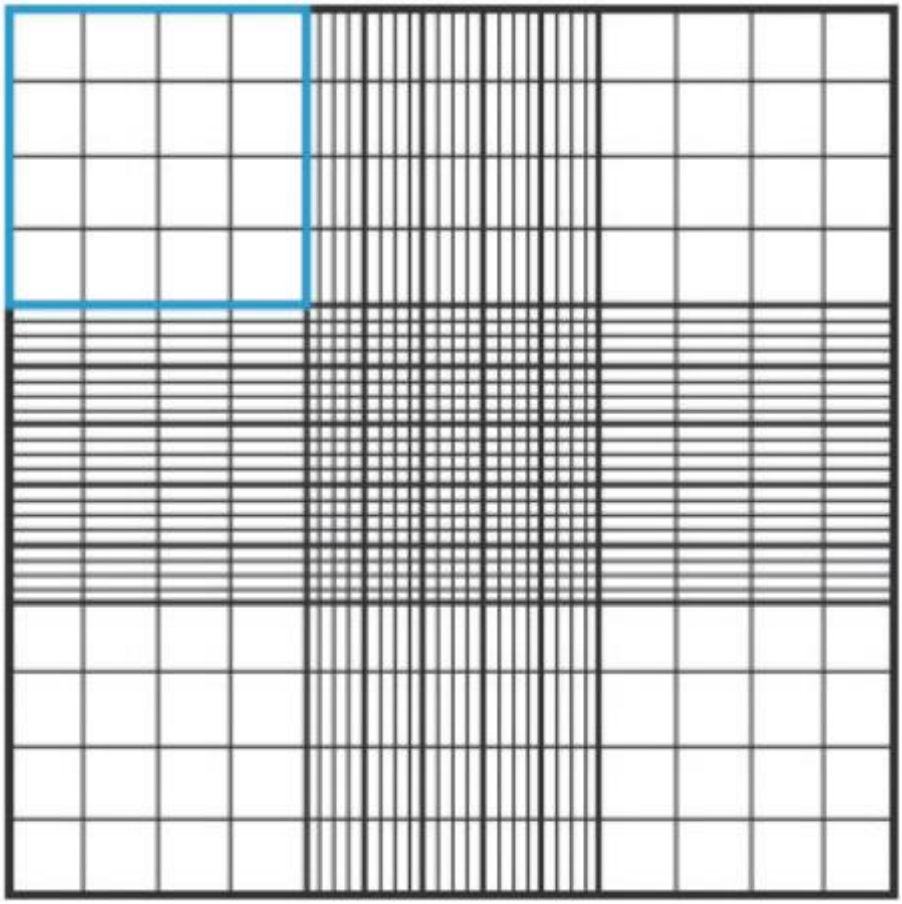

Figure 4.7: Hemocytometer counting chamber. Marked in blue is the set of 16 counting squares, cells laying inside this set of squares must be counted.

If the cell concentration differs from the one needed to perform the experiments, the adjustment can be calculated by the following equation:

$$C_1V_1 = C_2V_2 \quad (4.2)$$

where C_1 and V_1 are the initial concentration and volume, respectively, and C_2 and V_2 the desired concentration and volume, respectively. In case the concentration needs to be decreased, fresh growth medium is added until reaching the desired concentration. If the concentration needs to be increased, the suspension is centrifuged at 1500 rpm for 15 min, decanted and cell pellet re-suspended in the required amount of fresh medium. Once the cells suspensions with the desired concentrations were obtained, cells were loaded to tygon tubes, and connected to a device inlet on one end and to a manual valve on the other end, this valve could switch a pressurized line at 2.5 psi.

4.4.6 Cell trapping

Cell suspensions at 0.5, 1, 2.5, and 6 x10^6 cells/mL were loaded into new chips using medical grade tubes. These tubes were connected to a valve that switched the compressed air supply on one end and to the microfluidic chip on the other end. The chips were then mounted on an inverted fluorescence microscope and the exceeding tubing was placed flat on the microscope stage. A tile acquisition experiment was set on the Zen software to take micrographs only at the assay chambers coordinates on the stage. These images were taken with a 10x objective in the bright field channel with 0.25 µs exposure time. A time-lapse experiment was set in tandem with the tile acquisition. The time-lapse enables the acquisition of micrographs every 2 min for a total of 30 min. On the other hand, the tile set up permits image acquisition of only the assay chamber areas, without the need to scan the whole chip.

4.5 Biosensor experiments

These experiments considered the MITOMI-based biosensor. The button was designed to be used as a protein detection method based on a sandwich immunoassay. In this subsection we provide an account of the experimental setup that was mounted to perform, both, a general MITOMI immobilization of capture antibodies and a proof-of-concept immunoassay using enhanced green fluorescent protein (EGFP).

4.5.1 MITOMI button functionalization

The MITOMI buttons were pressurized by actuating the solenoid valve in the control panel that connects to their control line. A 3% bovine serum albumin (BSA) (A9647, Sigma-Aldrich Co.) in casein (37582, Thermo Fisher Scientific Inc.) solution was flowed for 15 min followed by a wash step with PBS for 5 min. Biotinylated BSA (29130, Thermo Fisher Scientific Inc.) at 200 µg/mL was perfused for 15 min and washed with PBS for 5 additional min. Next, DyLight 650 conjugated neutravidin (NA650) (84607, Thermo Fisher Scientific Inc.) was injected at a concentration of 1 µg/mL for 15 min and washed again with PBS for 5 min. If the labeled neutravidin was properly immobilized, a red fluorescent spot (Filter set 43, Carl Seizz) was visible under the MITOMI button. After the NA650 immobilization, biotin-conjugated antibodies for the cytokine of interest can be perfused into the chip at a desired concentration.

4.5.2 Proof-of-concept sandwich immunoassay

A proof-of-concept immunoassay must be performed, in order to test if the MITOMI button could serve as a biosensor for the detection of secreted proteins. For this purpose, an immunoassay using enhanced green fluorescent protein (EGFP) was carried out on the chip.

When NA650 was immobilized under the MITOMI button, through the protocol described in the previous section, biotinylated anti-GFP (Clone:5F12.4, eBioscience, Inc.) antibodies were perfused into the device at 4 µg/mL concentration for 15 min. A wash step with PBS 1x for 5 min followed. Once capture antibodies were immobilized, a 600 nM EGFP (4999, BioVision Incorporated, Milpitas, CA, USA) solution was delivered to the chip for 5 min, trying to simulate cytokine secretion from a captured cell population after stimulation. Protein binding to antibodies was confirmed by the visualization of co-localized fluorescent spots under the MITOMI button in the red and green (Filter set 38 HE, Carl Zeiss) channels, for NA650 and EGFP respectively.

A detection antibody solution of phycoerythrin (PE) conjugated anti-GFP (IC4240P, R&D Systems, Inc.) antibodies were perfused into the device and washed after 15 min. This antibody binds to different epitopes in the protein [60] and will signal the localization of immobilized EGFP in the chamber when watched in the orange channel (Filter set 50, Carl Zeiss).

4.6 Chapter summary

In this chapter, we provided a detailed account of the methodology employed in order to fabricate the microfluidic device. This fabrication process uses photolithography techniques for mold fabrication, and soft lithography techniques for replica molding. We also explained how the experimental setup was done, from cell culturing to cellular suspension preparation, and the way the cell patterning experiments were performed. Additionally, the functionalization of the biosensing element was described, as well as the experimental procedure for a proof-of-concept immunoassay.

5 Results

5.1 Chip characterization

Using the first replicas made from the micro patterned molds, a few parameters were characterized for both molds. First, we measured the height of the different structures in the chip. Next, we performed a test of the chamber isolation mechanisms to see, if in fact, up to four different conditions could be generated in one chip. The resulting chip can be seen in figure 5.1.

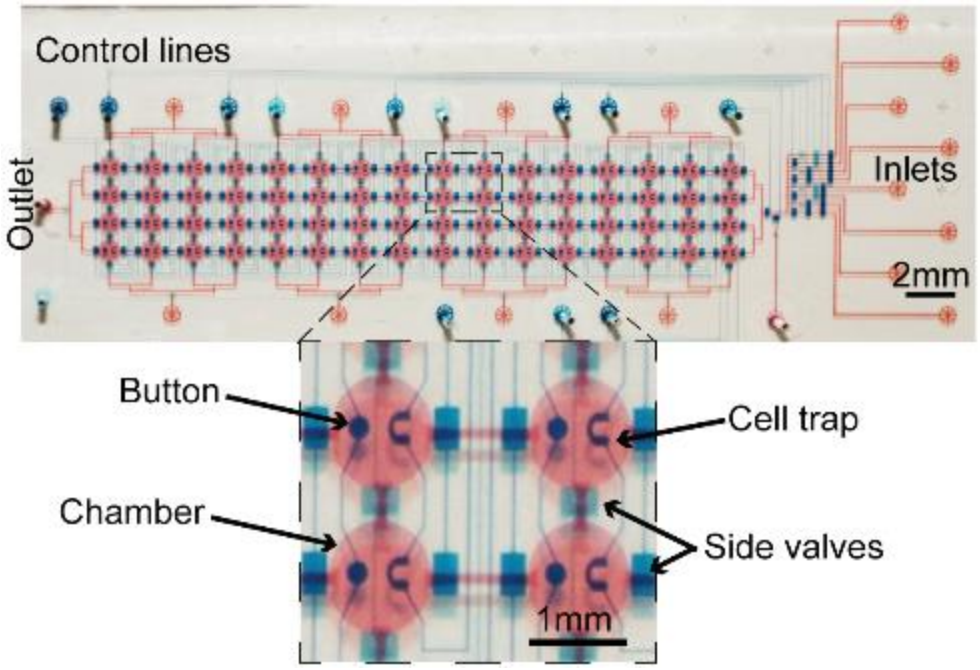

Figure 5.1: Photograph of the final chip. A blue colored water was injected to the control layer and a red colored solution to the flow layer.

5.1.1 Height measurement

The first parameter we characterized was the height of the different structures. Replica PDMS chips were cut in a cross sectional fashion at several points along its length and placed on top of a glass slide, then mounted on the

inverted microscope. Micrographs were acquired and measurements were taken using the microscope software (ZEN, Carl Zeiss Microscopy GmbH). The final heights, shown in table 5.1, were the result of measuring 4 different structures for each photoresist employed from 2 different chips. The obtained height of the chamber (14-µm) ensures a monolayer cell pattern, since the size of monocytes ranges between 9 to 17 microns [61], the dimension of the chamber prevents the cells from overlapping. The final flow channel height was greater than the intended 20-µm height we aimed for. The reason behind this, is that positive photoresist does not cross-link, and during the reflow step it melts. This melting, makes the structures shrink from the sides and raise vertically due to surface tension and the surface properties of the wafer [62]. The height of the control channels, although being lower than what it was expected, did not seem to affect the overall performance of the control layer, as it will be appreciated in the following sections.

Structure	Mean height [µm]	S.D.
Assay chamber	14.04	1.35
Flow channel	30.96	0.81
Control channel	18.59	1.09

Table 5.1. Final heights for each structure.

5.1.2 On-chip stimuli delivery

We designed the device such that up to four different stimuli conditions could be delivered to the assay chambers, with a total of 16 chambers subjected to the same condition. We can create four subsections by actuating the chambers lateral valves, while keeping the bottom and top valves unactuated. This inhibits flow from the common inlet to the common outlet. However, four paths open enabling fluid flow from the stimuli inlets to the stimuli outlets. We were able to introduced four different

food coloring solutions to the device and no cross-contamination between them was observed, as shown in Figure 5.3.

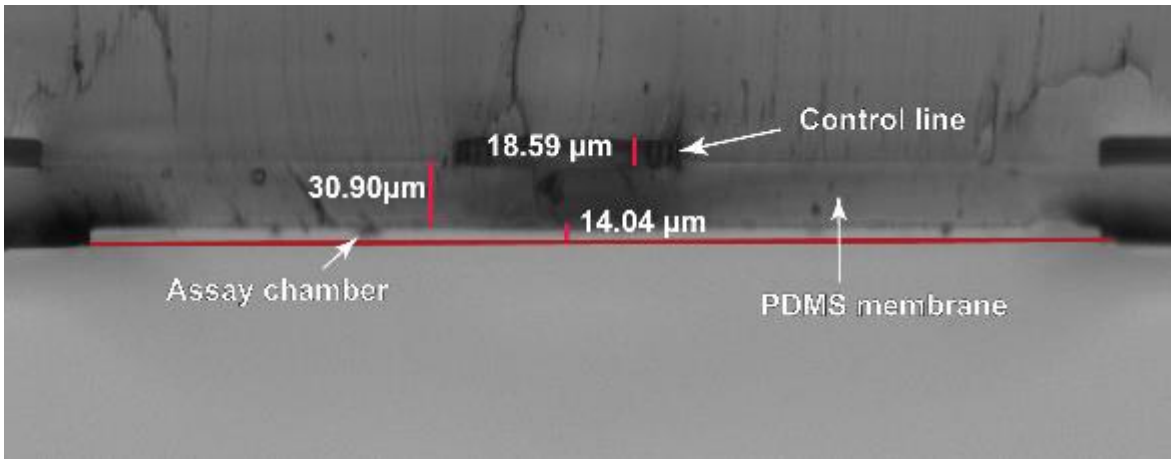

Figure 5.2: Cross sectional cut of the PDMS chip, showing the mean height for each structure.

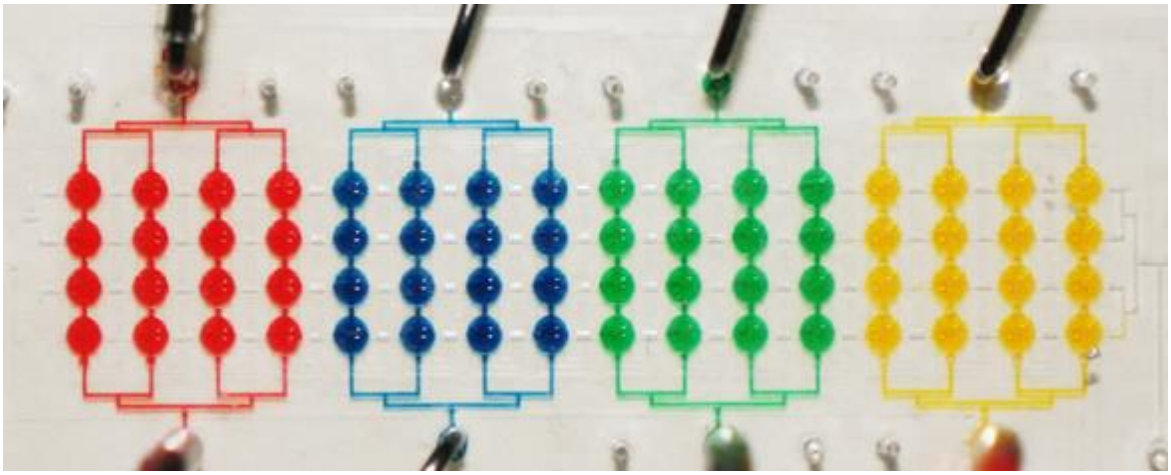

Figure 5.3: On-chip delivery of four different stimuli test. The side valves were closed and different colored solution were introduced through the stimuli inlets. The valves show proper isolation by inhibiting solution mixing.

5.1.3 C-cup contact area

The contact area between the PDMS membrane under the c-cup control line, and the glass slide was also characterized. This step was done by flowing a

fluorescent molecule called fluorescein isothiocyanate (FITC) into the chip at a 10 µM concentration. The solution was loaded at 2.5 psi, until no air remained trapped in the flow layer. Next, the c-cups' control line was pressurized from 0 to 25 psi in 5 psi increments. Fluorescent images were taken in the green channel (Filter set 38 HE, Carl Zeiss) under the inverted fluorescence microscope, with a 10x objective and an exposure time of 1000 ms.

The c-cup is deformed when the line pressure is increased: the PDMS membrane deflects into the assay chamber, displacing fluorescent molecules, thus decreasing its fluorescent intensity, exemplified in Figure 5.4. If this intensity is indistinguishable from the background, it means that the membrane is making full contact against the glass slide.

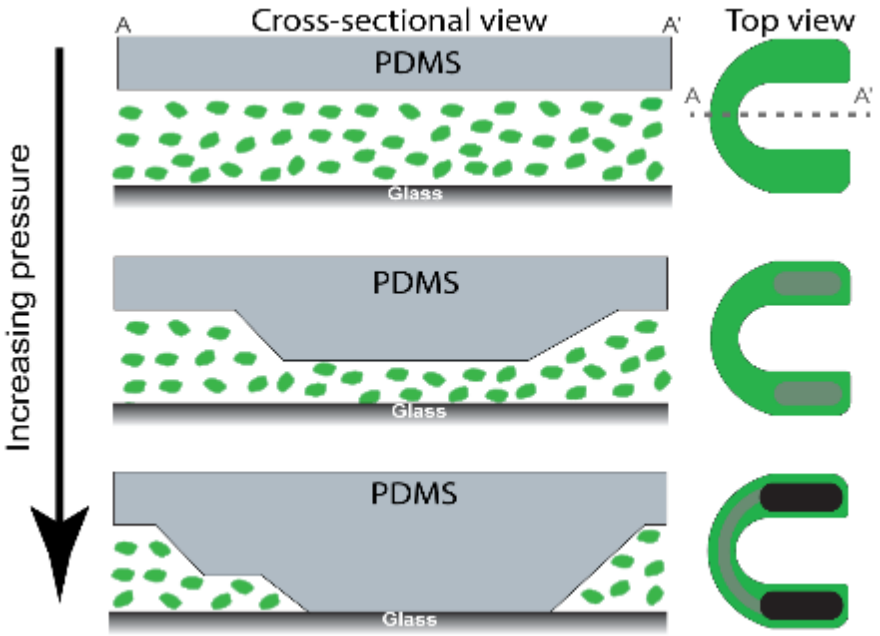

Figure 5.4: Schematic representation of fluorescent molecules displaced from the chamber when the PDMS membrane is actuated at increasing pressures.

Because the c-cup width is not uniform, the wider sides start to deflect at lower pressures compared to the narrow section, as is shown in Figure 5.5 (more

obvious at 10 psi to and 15 psi). Taking advantage of this behavior the line pressure can be modulated, giving rise to a reversible weird trap on the back, while the c-cups sides, give rise to walls that prevent cell dislodging in each assay chamber.

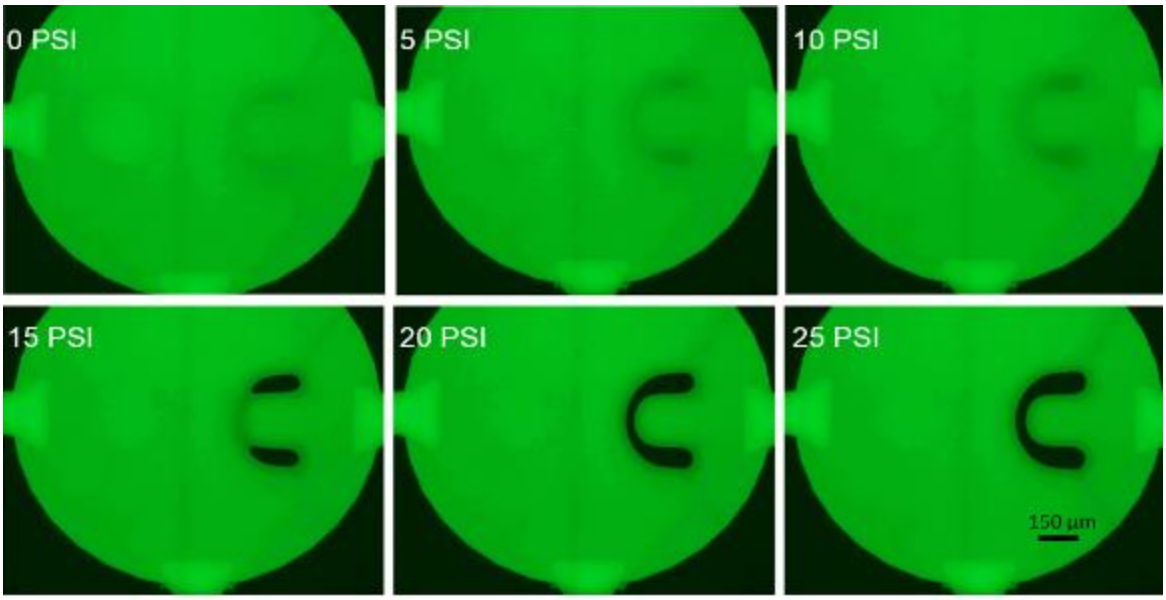

Figure 5.5: Representative image of a c-cup contact area at six different pressures with the device filled with FITC. When pressure is applied to the c-cup control line, the PDMS membrane deflects into the chamber space, displacing fluorescent molecules, thus observing a decrease in the fluorescence intensity. When the PDMS membrane comes in contact with the glass, the fluorescence under the c-cup disappears. At 15 psi, for example, it can be observed that a weir forms at the back of the trap, by noticing a lower level of fluorescence intensity; while the sides of the c-cup generate walls, inferred by the black area on the top and bottom portions.

5.2 Cell capture and protein sensing characterization

In the next subsection, we present and discuss the results that were obtained for both, the cell patterning method and the biosensor.

5.2.1 Cell patterning

Cells were loaded into the device at various concentrations with a driving pressure of 1.5 psi, meanwhile c-cups were pressurized at 21 psi. The top and bottom valves in the chambers were also pressurized at 24 psi, allowing only lateral flow throughout the chip. Micrographs in bright field were taken every two min under an inverted microscope and the number of cells counted.

The experiments carried out confirm that we can mechanically regulate the size of cellular populations patterned in the assay chamber to eventually study their protein secretion response after a specific stimulus. Figure 5.6 shows a representative c-cup being filled over time with cells.

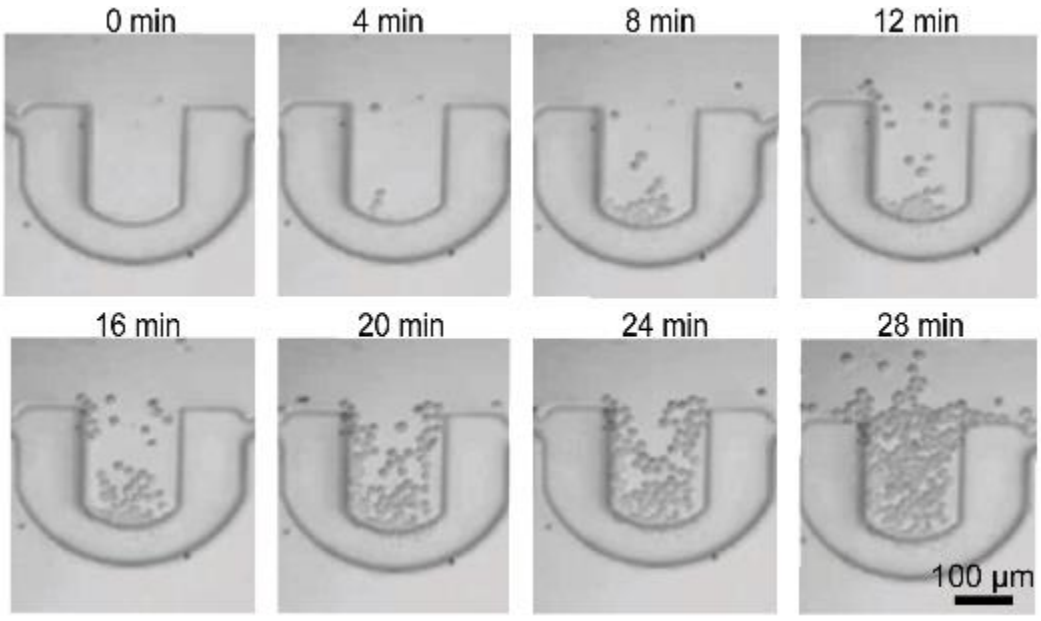

Figure 5.6: Representative c-cup being filled over time using a 2.5x10^6 cells/mL concentration. The number of trapped cells increased with seeding time.

Three experiments using different chips were conducted for each cell suspension concentration, the number of trapped cells were counted manually, with the help of a MATLAB (R2014a, Mathworks) script, that cropped all the images

around the c-cup and inserted grid lines every 50 pixels (Appendix A); and a clicker application, developed in C#. The counting was done for each instant of time and the mean and standard deviation of captured cells for each concentration were plotted. As we can see from Figure 5.7, the device provides a quantitative and high-throughput method for cell capture by regulating both, the cell concentration and the cellular seeding times.

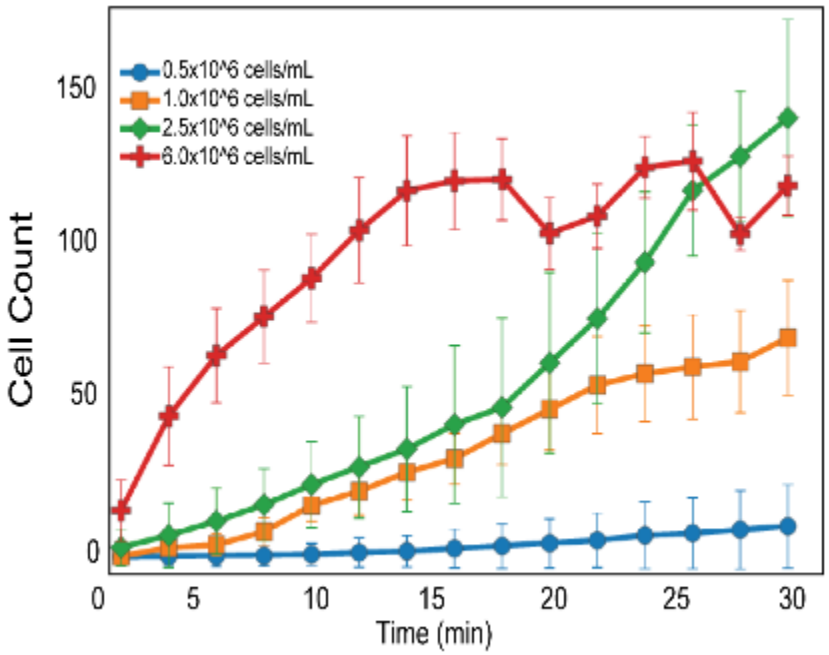

Figure 5.7: Captured cell count versus time for four different concentrations.

When using a high concentration of cells ($6x10^6$ cells/mL), it was noticed that the c-cups were completely filled within 18 min after cell seeding. When the c-cups were fully filled, incoming cells could dislodge cell clumps and the space left would in turn be filled with cells until more cells clumps where dislodged again. This effect gave rise to an oscillatory pattern for this specific concentration. Figure 5.8 shows a representative c-cup exhibiting this behavior.

Cells that remained in the assay chamber but outside the c-cup, provide a non-controllable amount of cells to the population isolated in an assay chamber (Figure 5.9a). Thus, fresh growth medium must be perfused for 5 min in order to wash away undesired cells (Figure 5.9b). We noted that after this wash step ~15 cells remained in the chamber, while a reduction of cells in the trap was observed (~25 cells).

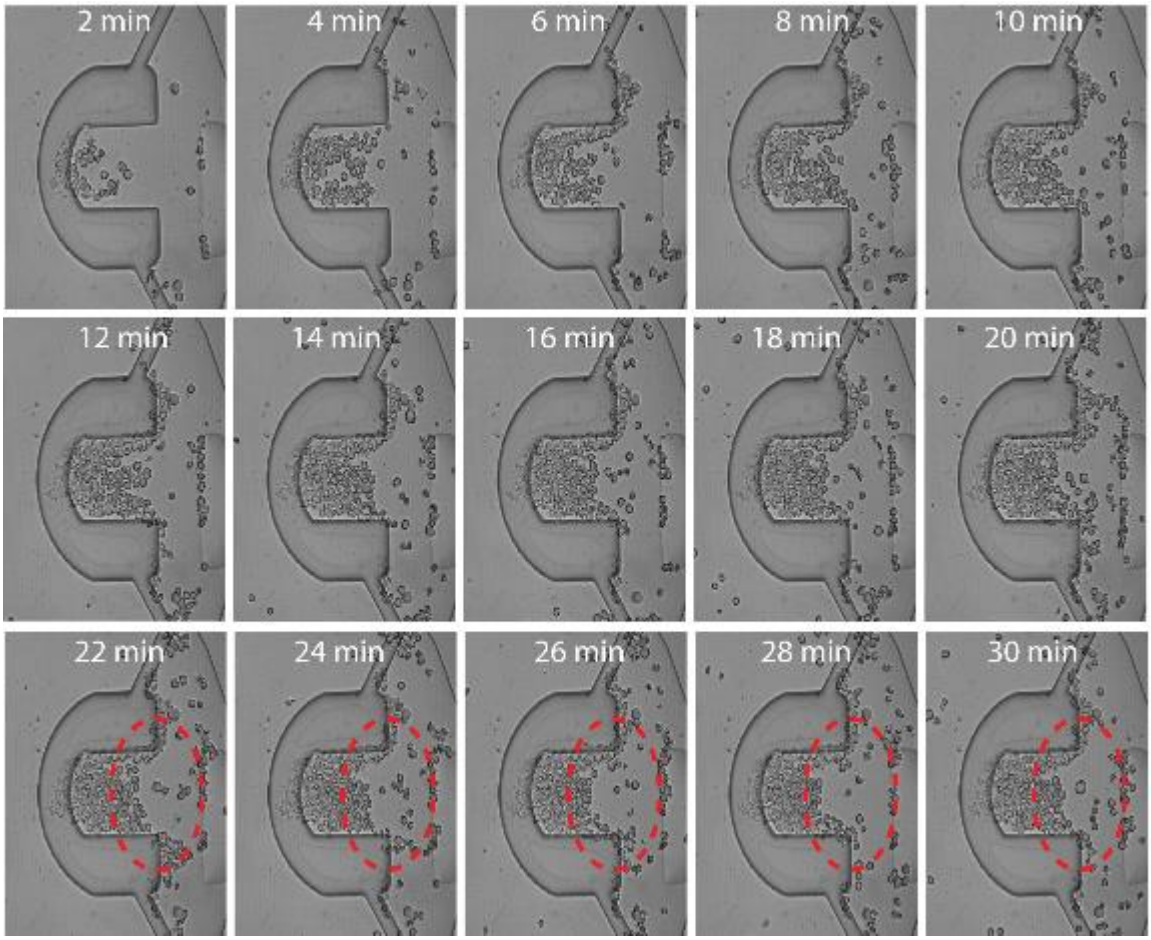

Figure 5.8: Representative c-cup being filled over timer using a 6x10^6 cells/mL concentration. The dashed circles showed an area which is filled with cells at 22 min. At 24 min it can be observed that cells were displaced; however, by min 30 incoming cells are starting to fill again the empty area.

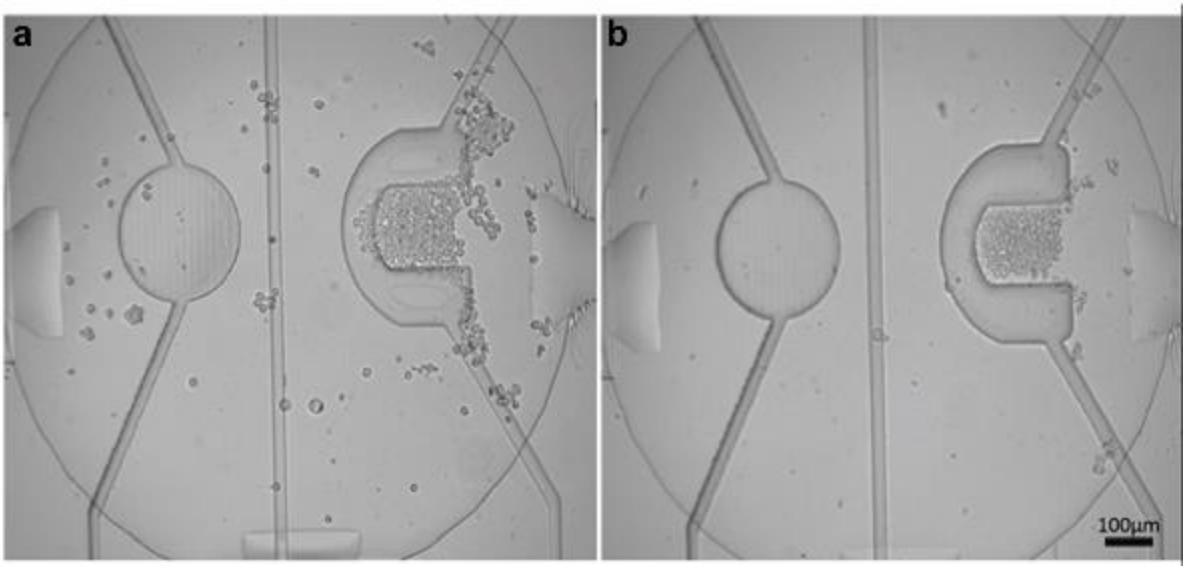

Figure 5.9: Excess cells in chamber. a) Chamber after cell loading, showing an uncontrollable amount of cells in the chamber. b) After the chamber wash step with fresh growth medium, most of the cells outside the trap could be removed.

BSA has also been shown to deter cell attachment [64], meaning that the passivation layer for the MITOMI button functionalization also serves the purpose of reducing the number of unregulated cells left in the assay chambers.

5.2.2 Proof-of-concept immunoassay

A proof of concept immunoassay with enhanced green fluorescent protein was carried out to test the biosensing capabilities of the MITOMI button. First, capture antibodies were immobilized under the MITOMI button, exemplified in figure 5.10. The immobilization was carried out by pressurizing the MITOMI button at 24 psi, ensuring maximal contact area between the PDMS membrane and the glass. A blocking solution was then delivered to the chip and washed. Next, pressure from the MITOMI buttons was released and biotin conjugated BSA was flowed, which physisorbes to the unblocked glass. Fluorescently label neutravidin (NA650) was then delivered to the chip, this molecule binds to the biotin due to their great affinity.

After washing the remaining NA650, biotinylated anti-GFP antibodies were injected for 15 min and washed; the biotin side of the antibodies bind to the remaining binding sites of the NA650.

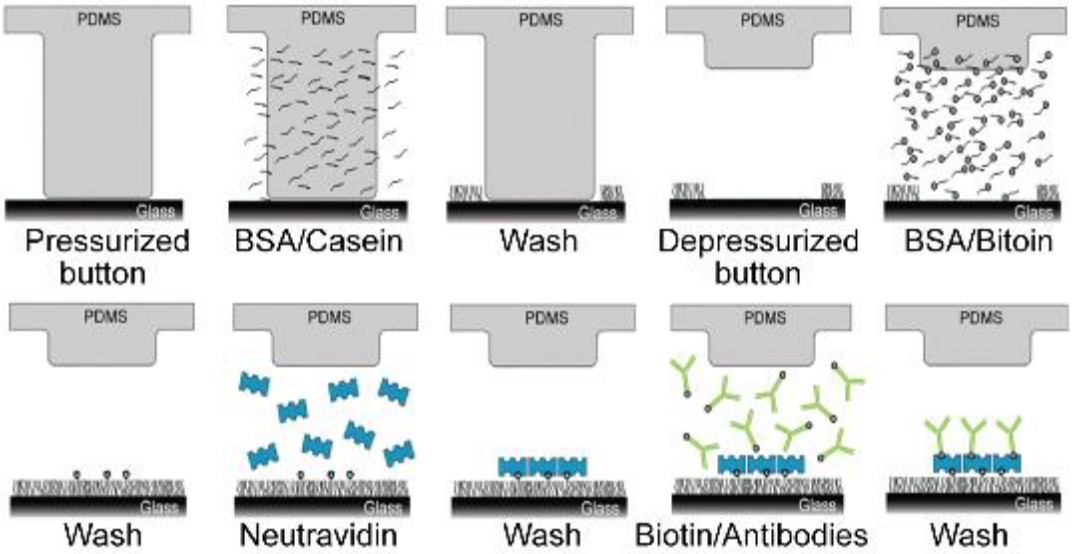

Figure 5.10: Schematic representation of the capture antibodies immobilization procedure.

Next, EGFP was perfused through the chip, the immobilized capture antibodies bind to and epitope in the protein. After washing remaining EGFP, a solution with PE conjugated anti-GFP antibodies was flowed. The detection antibodies bind to different epitopes on the immobilized protein. After the immobilization of all the molecules, micrographs were acquired at 1000 ms exposure time for both the NA650 and PE channel and 1800 ms for the EGFP channel. As shown in Figure 5.11, fluorescent spots were co-localized under the MITOMI button, suggesting the properly assembly of the immunocomplex.

With the use of a MATLAB script, homogeneity of the spot intensities across the device was measured (Figure 5.12). Observing a uniform distribution in the final intensities for both the NA650 and PE channels; however, great variability was shown under the GFP channel final intensities. GFP is a protein known to have a

tendency to aggregate itself [65], immobilization of random size aggregates could lead to the variability in its final intensity. While the reason that the PE channel does not show a similar variability, could be the fact that, even though the protein aggregates were immobilized by the capture antibodies, not all of the epitopes are available for binding to the detection antibodies. These epitopes remain hidden inside the protein aggregates, where detection antibodies cannot reach them.

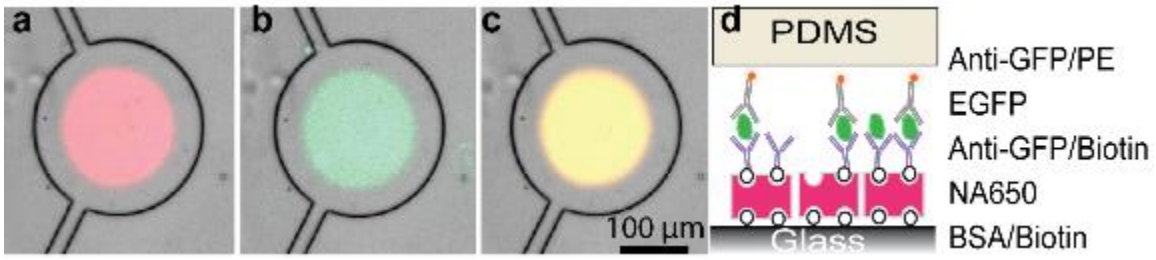

Figure 5.11: Proof of concept immunoassay with EGFP. Representative MITOMI button, showing colocalization of fluorescent spots in the a) NA650, b) EGFP, and c) PE channels. d) Schematic showing the structure of the immunocomplex. Biotinylated BSA is physisorbed on the glass under the MITOMI button. Neutravidin, which presents great affinity for biotin, binds to the immobilized BSA. Biotinylated antibodies attach to the remaining neutravidin binding sites. Fluorescently labeled antibodies bind to a different part of the same protein, indicating the presence of this molecule.

5.3 Chapter summary

In this chapter, we presented the results obtained during the thesis. We were able to design and fabricate a microfluidic device that consisted of 64 assay chambers. Each chamber incorporated both a trapping and a bio-sensing mechanism that used pneumatic pressure in order to be actuated. Also an on-chip stimuli delivery was integrated to the device allowing up to four different conditions to be maintained. The final height of the culture chambers, enabled the formation of

a monolayer of captured cells, helping obtain a more homogeneous number of trapped cells per c-cup. We were able to trap THP-1 cells, with the number of trapped cells increasing in function of cell concentration and seeding times. Furthermore, we were able to perform a proof-of-concept immunoassay using GFP, simulating protein secretion from a trapped cell population.

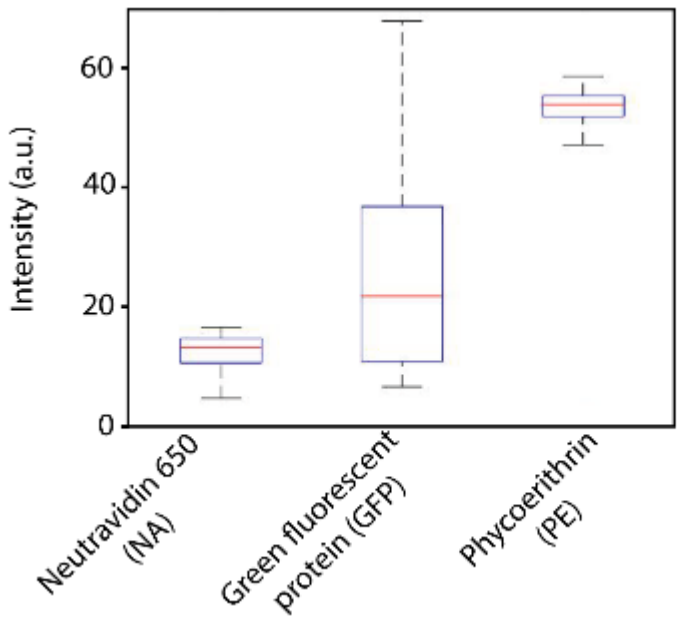

Figure 5.12: Final intensities for the three fluorescent channels, showing a homogenous intensity for both the NA and the PE channels, while GFP shows a non-uniform distribution. Red lines represent the mean intensity values, the box edges the 1st and 3rd median quartile, while bars delimit the maximum and minimum values.

6 Discussion

Although microfluidic approaches have been previously reported to quantitate cytokine secretion, most of these devices [23, 50, 51] utilize a single cell approach. Compared to these strategies, the device here reported, is capable of isolating a defined cell population, with the main advantage that it opens up the possibility to test population dependent protein secretion, a capability that may be useful for broad intercellular communication studies.

When compared to devices that assay cell secretion at the low ensemble level, our device provides two main advantages from previously reported devices [54, 55]. First, on-chip stimulation is enabled in our device, a feature lacking in the reported devices where cells are stimulated off-chip, and then introduced and isolated in the device, providing a single condition per device. Our device makes possible to have up to four different conditions for cell stimulation. Second, the cell patterning method employed, permits the integration of the structures for such purpose in the control layer. Although this fact makes manufacturing of the device easier, it could also be disadvantageous, since a previous cell purification step must be performed when working with primary cells, in order to isolate a desired cell line from a heterogeneous mix, such as blood. However, assays utilizing immortalized cell lines overcome this hurdle.

When relating the cell capture efficiency results to those previously reported by Liu and collaborators, we are able to obtain cell capture numbers and standard deviations similar to them. However, actuating pressures and flow rates do not agree with their results. The reason behind this could be small differences in the trap design, PDMS membrane thickness, assay chamber design and final height. While the high variability showed in the number of trapped cells, where the maximum coefficient of variation is around 23%, falls in value ranges previously reported of

variation for different cell counting methods [66], such as the hemocytometer. Where the large variations arise from error inducing situations presented to the user performing the count, such as cells lying on the gridlines, debris and cell clusters. These errors can be produced when preparing the cell seeding suspensions and during the actual count of cells immobilized in the traps, all adding up to the variability in the number of trapped cells. Although these same variation is observed in the work published by Liu, the author states that this particular method is a quantitative approach for high-throughput cell patterning in microfluidic devices.

7 Conclusions

In this thesis the integration of a cell trapping mechanism together with an immuno-based biosensor in a microfluidic device was presented. Both of the strategies employed pneumatically actuated structures. This facilitated their implementation by placing both structures in the same layer. Moreover, valves for fluid control were accommodated in the control layer.

The end result was a PDMS device with 64 assay chambers, in which up to 4 different stimuli can be delivered. We were able to trap monocytes, and showed that the number of captured cells in the traps increased as a function of, both, seeding time and cellular concentration. Regulating the amount of cells captured in a trap, enables the study of the protein secretion dependent on population size. Cell titrations, for example, are experiments where different concentrations of cells are tested in order to determine which concentration is optimal for a particular assay and detection system. The cell concentration that should be used for further assays, is selected based on the linear relationship between the detection signal and the number of cells [67]. If the detection signal does not scale linearly with the cell concentration used, this cell concentration should not be employed. For this reason, our device could be used for rapid cell titrations in secretome assays.

Furthermore, a proof-of-concept immunoassay was performed in the device using GFP. The experiments suggest that the immunocomplex under the MITOMI button is forming in a proper manner. The fluorescence intensities shown by the detection antibodies were uniform across all buttons; this validated our approach as a protein bio-sensing application.

8 Perspectives

As future work, experiments with stimulated cells and immobilized anti-cytokine antibodies must be conducted, in order to test if the device can indeed detect proteins secreted from the captured cell population. Also a better characterization of the bio-sensing element must be achieved. Although the MITOMI button has been proven to obtain sensibilities comparable to the gold standard ELISA (in the order of pg/mL) it is still unknown if this limit of detection is below the estimated secretion level of the maximum sized cell population isolated in the assay chambers. In case this is not accomplished, there are two possible solutions, either increasing the area of the cell trap or decreasing the volume of the assay chambers in order to concentrate the secreted proteins.

Furthermore, the device design can be improved. Purge outlets and valves can be incorporated to the stimuli inlets, in order to provide a better method for air purging when stimuli are delivered. Air pockets hinder the proper functioning of microfluidic devices; furthermore, if air enters the assay chambers, the molecules immobilized under the MITOMI button, might lose their bioactivity [39].

In addition, through minor changes in the design a second multiplexer can be integrated in order to address individual rows of assay chambers. This would enable the opportunity of isolating different cell lines in each row. Cell co-culture capabilities will allow broader cell-cell communication studies, by observing the effect of a stimulated cellular population over a contiguous one, by only allowing diffusion of soluble factors between adjacent chambers.

Not only immunological studies can be carried out in the chip presented in this thesis, but cancer biological studies could also be performed. The release of exosomes has been recently shown to be a major form of cell-cell communication mechanism between cancerous cells [68]. The MITOMI button enables the

immobilization of exosome marker antibodies; in this case, it could be possible to correlate the amount of exosome release to the metastatic potential of a tumor, while drugs can be tested that diminish this effect.

9 References

[1] Alberts B, Johnson A, Lewis J, et al. Molecular Biology of the Cell. 4th edition. New York: Garland Science; 2002. General Principles of Cell Communication.

[2] Cozzolino, F., Torcia, M., Aldinucci, D., Ziche, M., Almerigogna, F., Bani, D., & Stern, D. M. (1990). Interleukin 1 is an autocrine regulator of human endothelial cell growth. *Proceedings of the National Academy of Sciences*, 87(17), 6487-6491.

[3] Bellve, A. R., & Zheng, W. (1989). Growth factors as autocrine and paracrine modulators of male gonadal functions. *Journal of reproduction and fertility*, *85*(2), 771-793.

[4] Fang, F. C., & Casadevall, A. (2011). Reductionistic and holistic science. *Infection and immunity*, *79*(4), 1401-1404.

[5] Coico, R., & Sunshine, G. (2015). *Immunology: a short course*. John Wiley & Sons.

[6] Hames, A. D., Rickwood, D., & Delves, P. J. (2014). *Cellular Immunology Labfax*. Elsevier.

[7] Zhang, J. M., & An, J. (2007). *Cytokines, inflammation and pain. International anesthesiology clinics*, 45(2), 27.

[8] Hodgkin, P. D., Rush, J., Gett, A. V., Bartell, G., & Hasbold, J. (1998). The logic of intercellular communication in the immune system. *Immunology and cell Biology*, 76(5), 448-453.

[9] Garlanda, C., Dinarello, C. A., & Mantovani, A. (2013). *The interleukin-1 family: back to the future. Immunity*, 39(6), 1003-1018.

[10] Wajant, H., Pfizenmaier, K., & Scheurich, P. (2003). Tumor necrosis factor signaling. *Cell Death & Differentiation*, 10(1), 45-65.

[11] Groves, D. T., & Jiang, Y. (1995). Chemokines, a family of chemotactic cytokines. Critical Reviews in Oral Biology & Medicine, 6(2), 109-118.

[12] Egli, A., Santer, D. M., O'shea, D., Tyrrell, D. L., & Houghton, M. (2014). The impact of the interferon-lambda family on the innate and adaptive immune response to viral infections. Emerging Microbes and Infections, 3, 51.

[13] Mazurek, G. H., Jereb, J., LoBue, P., Iademarco, M. F., Metchock, B., & Vernon, A. (2005). Guidelines for using the QuantiFERON-TB Gold test for detecting Mycobacterium tuberculosis infection, United States. *MMWr recomm rep*, *54*(RR-15), 49-55.

[14] Dranoff, G. (2004). Cytokines in cancer pathogenesis and cancer therapy. *Nature Reviews Cancer*, *4*(1), 11-22.

[15] *Thermo Scientific Pierce Assay Development Technical Handbook. Thermo Fisher Scientific, (2011).*

[16] *Aziz, N., Nishanian, P., Mitsuyasu, R., Detels, R., & Fahey, J. L. (1999). Variables that affect assays for plasma cytokines and soluble activation markers. Clinical and diagnostic laboratory immunology, 6(1), 89-95.*

[17] Brown, M., & Wittwer, C. (2000). Flow cytometry: principles and clinical applications in hematology. *Clinical chemistry*, *46*(8), 1221-1229.

[18] Amir, E. A. D., Davis, K. L., Tadmor, M. D., Simonds, E. F., Levine, J. H., Bendall, S. C., & Pe'er, D. (2013). viSNE enables visualization of high dimensional single-cell data and reveals phenotypic heterogeneity of leukemia. *Nature biotechnology*, *31*(6), 545-552.

[19] Streets, A. M., & Huang, Y. (2013). Chip in a lab: Microfluidics for next generation life science research. *Biomicrofluidics*, *7*(1), 011302.

[20] Smith, S., Moodley, K., Govender, U., Chen, H., Fourie, L., Ngwenya, S., & Potgieter, S. (2015). Paper-based smart microfluidics for education and low-cost diagnostics. *South African Journal of Science*, 111(11-12), 1-10.

[21] Cesaro-Tadic, S., Dernick, G., Juncker, D., Buurman, G., Kropshofer, H., Michel, B., & Delamarche, E. (2004). High-sensitivity miniaturized immunoassays for tumor necrosis factor α using microfluidic systems. *Lab on a Chip*, *4*(6), 563-569.

[22] Liu, K. K., Wu, R. G., Chuang, Y. J., Khoo, H. S., Huang, S. H., & Tseng, F. G. (2010). Microfluidic systems for biosensing. *Sensors*, 10(7), 6623-6661.

[23] Shirasaki, Y., Yamagishi, M., Suzuki, N., Izawa, K., Nakahara, A., Mizuno, J., & Ohara, O. (2014). Real-time single-cell imaging of protein secretion. *Scientific reports*, *4*.

[24] Nickel, W. (2003). The mystery of nonclassical protein secretion. *European Journal of Biochemistry*, *270*(10), 2109-2119.

[25] Halldorsson, S., Lucumi, E., Gómez-Sjöberg, R., & Fleming, R. M. (2015). Advantages and challenges of microfluidic cell culture in polydimethylsiloxane devices. Biosensors and Bioelectronics, 63, 218-231.

[26] Gómez-Sjöberg, R., Leyrat, A. A., Pirone, D. M., Chen, C. S., & Quake, S. R. (2007). Versatile, fully automated, microfluidic cell culture system. *Analytical chemistry*, *79*(22), 8557-8563.

[27] Yin, B. S., Li, M., Liu, B. M., Wang, S. Y., & Zhang, W. G. (2015). An integrated microfluidic device for screening the effective concentration of locally applied tacrolimus for peripheral nerve regeneration. *Experimental and therapeutic medicine*, *9*(1), 154-158.

[28] Kane, R. S., Takayama, S., Ostuni, E., Ingber, D. E., & Whitesides, G. M. (1999). Patterning proteins and cells using soft lithography. *Biomaterials*, 20(23), 2363-2376.

[29] Chan, C. M., Ko, T. M., & Hiraoka, H. (1996). Polymer surface modification by plasmas and photons. *Surface science reports*, 24(1), 1-54.

[30] IUPAC. (1997). *Compendium of Chemical Terminology*, 2nd ed. Compiled by A. D. McNaught and A. Wilkinson. Blackwell Scientific Publications, Oxford

[31] Tourovskaia, A., Barber, T., Wickes, B. T., Hirdes, D., Grin, B., Castner, D. G & Folch, A. (2003). Micropatterns of chemisorbed cell adhesion-repellent films using oxygen plasma etching and elastomeric masks. *Langmuir*, 19(11), 4754-4764.

[32] Filipponi, L., Livingston, P., Kašpar, O., Tokárová, V., & Nicolau, D. V. (2016). Protein patterning by microcontact printing using pyramidal PDMS stamps. *Biomedical microdevices*, 18(1), 1-7.

[33] Desai, N. P., & Hubbell, J. A. (1991). Solution technique to incorporate polyethylene oxide and other water-soluble polymers into surfaces of polymeric biomaterials. *Biomaterials*, 12(2), 144-153.

[34] Gumbiner, B. M. (1996). Cell adhesion: the molecular basis of tissue architecture and morphogenesis. *Cell*, 84(3), 345-357.

[35] Thomas, C. H., Lhoest, J. B., Castner, D. G., McFarland, C. D., & Healy, K. E. (1999). Surfaces designed to control the projected area and shape of individual cells. *Journal of biomechanical engineering*, 121(1), 40-48.

[36] Chan, J. K. C., Ng, C. S., & Hui, P. K. (1988). A simple guide to the terminology and application of leucocyte monoclonal antibodies. *Histopathology*, 12(5), 461-480.

[37] Cheng, X., Irimia, D., Dixon, M., Sekine, K., Demirci, U., Zamir, L., & Toner, M. (2007). A microfluidic device for practical label-free CD4+ T cell counting of HIV-infected subjects. *Lab on a Chip*, 7(2), 170-178.

[38] Cox, J. C., & Ellington, A. D. (2001). Automated selection of anti-protein aptamers. *Bioorganic & medicinal chemistry*, 9(10), 2525-2531.

[39] Mumenthaler, M., Hsu, C. C., & Pearlman, R. (1994). Feasibility study on spray-drying protein pharmaceuticals: recombinant human growth hormone and tissue-type plasminogen activator. *Pharmaceutical research*, 11(1), 12-20.

[40] Rettig, J. R., & Folch, A. (2005). Large-scale single-cell trapping and imaging using microwell arrays. *Analytical chemistry*, *77*(17), 5628-5634.

[41] Di Carlo, D., Wu, L. Y., & Lee, L. P. (2006). Dynamic single cell culture array. *Lab on a Chip*, 6(11), 1445-1449.

[42] Kimmerling, R. J., Szeto, G. L., Li, J. W., Genshaft, A. S., Kazer, S. W., Payer, K. R., ... & Manalis, S. R. (2016). A microfluidic platform enabling single-cell RNA-seq of multigenerational lineages. *Nature communications*, 7.

[43] Liu, W., Li, L., Wang, J. C., Tu, Q., Ren, L., Wang, Y., & Wang, J. (2012). Dynamic trapping and high-throughput patterning of cells using pneumatic microstructures in an integrated microfluidic device. *Lab on a chip*, 12(9), 1702-1709.

[44] Çetin, B., & Li, D. (2011). Dielectrophoresis in microfluidics technology. *Electrophoresis*, 32(18), 2410-2427.

[45] Steubing, R. W., Cheng, S., Wright, W. H., Numajiri, Y., & Berns, M. W. (1991). Laser induced cell fusion in combination with optical tweezers: the laser cell fusion trap. *Cytometry*, 12(6), 505-510.

[46] Inglis, D. W., Riehn, R., Austin, R. H., & Sturm, J. C. (2004). Continuous microfluidic immunomagnetic cell separation. *Applied Physics Letters*, 85(21), 5093-5095.

[47] Grier, D. G. (2003). A revolution in optical manipulation. *Nature*, 424(6950), 810-816.

[48] Potáčová, A., Štossová, J., Burešová, I., Kovářová, L., Almáši, M., Penka, M., & Hájek, R. (2011). Sample processing and methodological pitfalls in multiple myeloma research. *klinická onkologie*, 18.

[49] Garcia-Cordero, J. L., & Maerkl, S. J. (2013). Multiplexed surface micropatterning of proteins with a pressure-modulated microfluidic button-membrane. *Chemical Communications*, 49(13), 1264-1266.

[50] Ma, C., Fan, R., Ahmad, H., Shi, Q., Comin-Anduix, B., Chodon, T., & Ribas, A. (2011). A clinical microchip for evaluation of single immune cells reveals high functional heterogeneity in phenotypically similar T cells. *Nature medicine*, 17(6), 738-743.

[51] Son, K. J., Rahimian, A., Shin, D. S., Siltanen, C., Patel, T., & Revzin, A. (2016). Microfluidic compartments with sensing microbeads for dynamic monitoring of cytokine and exosome release from single cells. *Analyst*, 141(2), 679-688.

[52] Franses, J. W., Drosu, N. C., Gibson, W. J., Chitalia, V. C., & Edelman, E. R. (2013). Dysfunctional endothelial cells directly stimulate cancer inflammation and metastasis. *International journal of cancer*, 133(6), 1334-1344.

[53] Cheng, A. K., Sen, D., & Yu, H. Z. (2009). Design and testing of aptamer-based electrochemical biosensors for proteins and small molecules. *Bioelectrochemistry*, 77(1), 1-12.

[54] Zhou, Q., Kwa, T., Gao, Y., Liu, Y., Rahimian, A., & Revzin, A. (2014). On-chip regeneration of aptasensors for monitoring cell secretion. *Lab on a Chip*, 14(2), 276-279.

[55] Chen, A., Vu, T., Stybayeva, G., Pan, T., & Revzin, A. (2013). Reconfigurable microfluidics combined with antibody microarrays for enhanced detection of T-cell secreted cytokines. *Biomicrofluidics*, 7(2), 024105.

[56] Ma, Y., Thiele, J., Abdelmohsen, L., Xu, J., & Huck, W. T. (2014). Biocompatible macro-initiators controlling radical retention in microfluidic on-chip

photo-polymerization of water-in-oil emulsions. *Chemical Communications*, 50(1), 112-114.

[57] *Rehydration of photoresists.* MicroChemicals GmbH. Rev. December 2013. Source: http://www.microchemicals.com/technical_information/photoresist_rehydration.pdf

[58] Kaur, G., & Dufour, J. M. (2012). Cell lines: Valuable tools or useless artifacts. *Spermatogenesis*, 2(1), 1-5.

[59] Jansky, L., Reymanova, P., & Kopecky, J. (2003). Dynamics of cytokine production in human peripheral blood mononuclear cells stimulated by LPS, or infected by Borrelia. *Physiological research*, 52(5), 593-598.

[60] Lipman, N. S., Jackson, L. R., Trudel, L. J., & Weis-Garcia, F. (2005). Monoclonal versus polyclonal antibodies: distinguishing characteristics, applications, and information resources. *ILAR journal*, 46(3), 258-268.

[61] Wang, S. Y., Mak, K. L., Chen, L. Y., Chou, M. P., & Ho, C. K. (1992). Heterogeneity of human blood monocyte: two subpopulations with different sizes, phenotypes and functions. *Immunology*, 77(2), 298.

[62] *Reflow of photoresist.* MicroChemicals GmbH. Rev. December 2013. Source: http://www.microchemicals.com/technical_information/reflow_photoresist.pdf

[63] Tan, J. L., Liu, W., Nelson, C. M., Raghavan, S., & Chen, C. S. (2004). Simple approach to micropattern cells on common culture substrates by tuning substrate wettability. *Tissue engineering*, 10(5-6), 865-872.

[64] Kawamura, R., Mishima, M., Ryu, S., Arai, Y., Okose, M., Silberberg, Y. R., & Nakamura, C. (2013). Controlled cell adhesion using a biocompatible anchor for membrane-conjugated bovine serum albumin/bovine serum albumin mixed layer. *Langmuir*, 29(21), 6429-6433.

[65] Krasowska, J., Olasek, M., Bzowska, A., Clark, P. L., & Wielgus-Kutrowska, B. (2010). The comparison of aggregation and folding of enhanced green fluorescent protein (EGFP) by spectroscopic studies. *Spectroscopy*, 24(3-4), 343-348.

[66] Hsuing, F., McCollum, T., Hefner, E., & Rubio, T. (2013). Comparison of Count Reproducibility, Accuracy, and Time to Results between a Hemocytometer and the TC20 Automated Cell Counter. *Bulletin 6003.* Rev B, 1-4.

[67] Baldwin, C. L., Antczak, D. F., & Winter, A. J. (1985). Cell titration assay for measuring blastogenesis of bovine lymphocytes. *Veterinary immunology and immunopathology*, 9(4), 319-333.

[68] Ludwig, A. K., & Giebel, B. (2012). Exosomes: small vesicles participating in intercellular communication. *The international journal of biochemistry & cell biology*, 44(1), 11-15.

Appendix

Appendix A: MATLAB script for time-lapse experiments image cropping

```
%This script crops the images generated by the time-lapse experiment
%around the c-cup area, adding gridlines to the cropped images for easier
%counting.

%The .m file must be saved in the directory where the images are stored

%Find all files with .jpeg extension in directory
imagefiles = dir('*.jpeg');
nfiles = length(imagefiles);

%For all the images found from the time lapse experiment

for ii=1:nfiles

%Get the images names
   currentfilename = imagefiles(ii).name;

%Find the images that belong to a particular assay chamber
%(In this case chamber 1)
   if ~isempty(strfind(currentfilename, 's1c'))

%Crop the image to a square 1100 by 1100 pixels starting from pixel 1400
%in x axis and pixel 500 in y axis

         im = imcrop(imread(currentfilename),[1400 500 1100  1100]);

%Add black lines every 50 pixels on both axis

         im(50:50:end,:,:) = 0;
         im(:,50:50:end,:) = 0;

%Save the cropped image in the directory with a .bmp file extension
        imwrite(im,strcat(currentfilename,'.bmp'));

     end
end
```